

Photoinduced Processes within Compact Dyads Based on Triphenylpyridinium-Functionalized Bipyridyl Complexes of Ruthenium(II)

Philippe P. Lainé,^{*,[a]} Ilaria Ciofini,^[b] Philippe Ochsenbein,^[c] Edmond Amouyal,^[d] Carlo Adamo,^[b] and Fethi Bedioui^[e]

Dedicated to Professor Jean-Pierre Launay on the occasion of his 61th birthday

Abstract: As an alternative to conventional charge-separation functional molecular models based on long-range ET within redox cascades, a “compact approach” has been examined. To this end, spacer elements usually inserted between main redox-active units within polyad systems have been removed, allowing extended rigidity but at the expense of enhanced intercomponent electronic communication. The molecular assemblies investigated here are of the P-(θ^1)-A type, where the θ^1 twist angle is related to the degree of conjugation between the photosensitizer (P, of {Ru(bpy)₃}²⁺ type) and the electron-acceptor (A). 4-*N*- and 4-*N*’,4’-*N*’-(2,4,6-triphenylpyridinio)-2,2’-bipyridine ligands (**A₁-bpy** and **A₂-bpy**, re-

spectively) have been synthesized to give complexes with Ru^{II}, **1-bpy** and **2-bpy**, respectively. Combined solid-state analysis (X-ray crystallography), solution studies (¹H NMR, cyclic voltammetry) and computational structural optimization allowed verifying that θ^1 angle approaches 90° within **1-bpy** and **2-bpy** in solution. Also, anticipated existence of strong intercomponent electronic coupling has been confirmed by investigating electronic absorption properties and electrochemical behav-

Keywords: conformational switching • density functional calculations • electron transfer • luminescence • molecular devices

ior of the compounds. The capability of **1-bpy** and **2-bpy** to undergo PET process was evaluated by carrying out their photophysical study (steady state emission and time-resolved spectroscopy at both 293 and 77 K). The conformational dependence of photoinduced processes within P-(θ^1)-A systems has been established by comparing the photophysical properties of **1-bpy** (and **2-bpy**) with those of an affiliated species reported in the literature, **1-phen**. A complementary theoretical analysis (DFT) of the change of spin density distribution within model [**1-bpy**(θ^1)]⁻ mono-reduced species as a function of θ^1 has been undertaken and the possibility of conformationally switching emission properties of P was derived.

Introduction

The search for new molecular devices capable of monitoring photoinduced electron transfers (PET) is at the cross-roads

of the works devoted to both molecular electronics and photochemical conversion of solar energy (including artificial photosynthesis and photovoltaic devices).^[1–3] One of the major goals, within the latter framework of research, is to


[a] Dr. P. P. Lainé
Laboratoire de Chimie et Biochimie Pharmacologiques
et Toxicologiques (CNRS UMR 8601)
Université René Descartes
45 rue des Saints Pères
75270 Paris Cedex 06 (France)
Fax: (+33) 142-868-387
E-mail: philippe.laine@univ-paris5.fr

[b] Dr. I. Ciofini, Prof. C. Adamo
Laboratoire d’Électrochimie et Chimie Analytique (CNRS UMR-7575)
École Nationale Supérieure de Chimie de Paris
11 rue Pierre et Marie Curie
75231 Paris Cedex 05 (France)

[c] Dr. P. Ochsenbein
Sanofi-Aventis, 371 rue du Professeur Blayac
34184 Montpellier Cedex 04 (France)

[d] Dr. E. Amouyal
Laboratoire de Chimie Physique (CNRS UMR 8000)
Université Paris-Sud, Bâtiment 350
91405 Orsay Cedex (France)

[e] Dr. F. Bedioui
Laboratoire de Pharmacologie Chimique
et Génétique (CNRS UMR-8151 + INSERM U-640)
École Nationale Supérieure de Chimie de Paris
11 rue Pierre et Marie Curie
75231 Paris Cedex 05 (France)

 Supporting information for this article is available on the WWW under <http://www.chemeurj.org/> or from the author: ¹H NMR spectra of complexes **1-bpy** and **2-bpy**.

achieve the formation of long-lived charge-separated (CS) states.^[2–5] Multicomponent systems built from a photosensitizer (P) covalently linked—normally via spacers^[6]—to suitably arranged electron-withdrawing (A) and/or electron-releasing (D) units, are well adapted for that purpose.^[1–8] In our effort to further compact these molecular devices^[9] and exert a more acute control over their intramolecular geometry,^[10] we have designed putative acceptor-dyads models (P–A), made of A group(s) *directly* attached to P (e.g. **1-tpy** and **1-bpy**; Figure 1). Removal of bridging insulators (spacers) to extend molecular rigidity was anticipated to be at the expense of an undesirable increase of the intercomponent electronic coupling, usually withdrawn by the use of saturated—but often flexible—spacers such as methylene fragments.^[11,12] However, in the present case, the selected 2,4,6-triphenylpyridinium (H_3TP^+ ; Figure 1) electron-acceptor group (A) owns the great asset of possessing two bulky phenyl substituents *ortho* to the $N_{pyridinium}$ atom connected to P. These rings are likely to prevent the pyridinium from adopting a coplanar conformation with the covalently linked photosensitizer, as for instance in the case of **1-tpy** (Figure 1).^[10] This pronounced steric hindrance, localized around the P–A linkage, is assumed to warrant the disruption of the conjugation between the connected subunits. In other words, the advised intercomponent *electronic decoupling*^[1,8,13] is expected to be produced by a so-called *geometrical decoupling*, thus playing the role usually fulfilled by saturated spacers^[14] (at least for what concerns the π – π contribution to the interaction, which is by far the larger one). A key molecular parameter is therefore the twist angle θ^1 that accounts for the conformation of the plane of the pyridinium ring of A with respect to that of the chromophoric ligand partaking in P (Figure 1). Here, this dihedral angle is expected to be almost orthogonal ($\theta^1 \approx 90^\circ$).

In previous studies,^[10] we have reported on the properties of such “compact dyads” (e.g. **1-tpy**; Figure 1) based on the ruthenium(II)–bis-terpyridyl complex ($[Ru(tpy)_2]^{2+}$; **0-tpy**) as a P unit. It has been shown that the strong intramolecular electronic coupling dramatically affects the photophysical behavior of the photosensitizer, up to make it a so weak primary electron donor in the excited state that an intramolecular PET was precluded.^[10a] In that case, A can be considered as a substituent of P rather than a true component of a P–A acceptor dyad. To circumvent this drawback, we reasoned that the adverse contribution of electronic coupling could be counterbalanced by using a primary light-triggered electron-donor (*P) stronger than $[Ru(tpy)_2]^{2+}$, namely the archetypal ruthenium(II)–tris-bipyridyl complex.^[11,15] It is thus expected that, despite the noticeable intramolecular interaction, the excited-state reducing strength of P will remain strong enough to initiate the transient reduction of A. Another advantage that could be taken of such a replacement stems from the fact that **0-bpy** is a much greater lumiphore than **0-tpy**, thus making the photophysical study easier to carry out. One of the goals of the present study is to verify the capability of **1-bpy** and maybe **2-bpy** species (Figure 1) to form $[P^+-A^-]$ CS state.

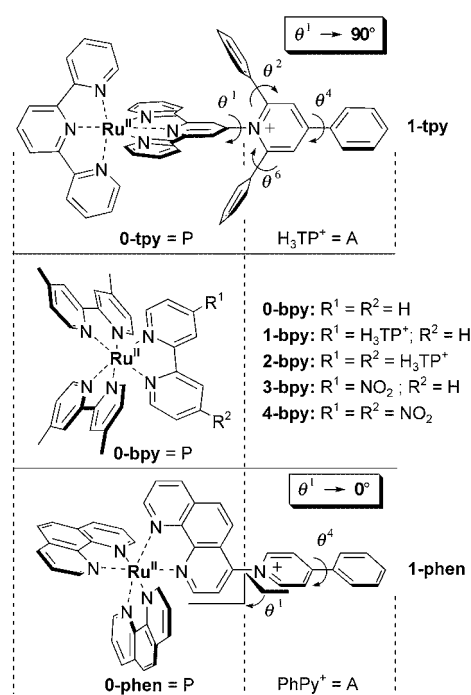


Figure 1. Schematic structures of the $[(Me_6bpy)_2Ru(bpyR^1R^2)]^{n+}$ together with reference $[(tpy)Ru(tpy-tph_3^+)]^{3+}$ and $[(phen)_2Ru(phen-PyPh^+)]^{3+}$ complexes along with their labels.

The present work is also aimed at investigating the critical degree of “electronic insulation” required to allow—or not—a directional inter-component process from *P to A such as PET, since there is no spacer to ensure the electronic integrity of the P and A subunits.^[16] Expectedly, the intercomponent electronic coupling can be modulated via a controlled intramolecular conformation,^[17–19] by simply changing the torsion angle ($0 \leq \theta^1 \leq 90^\circ$, Figure 1) between the P and A parts of the potentially fully conjugated molecule P–(θ^1)–A. The only parameter to be varied is then the actual degree of electronic conjugation of A with P. In this context, the photophysical properties of the **0-bpy**–**2-bpy** series of complexes are compared with those of an affiliated species (**1-phen**) previously described by Hupp and co-workers.^[20] Indeed, in **1-phen**, the *p*-phenylpyridinium A group ($PhPy^+$; Figure 1) is not sterically hindered, thus allowing the acceptor A and the phen ligand (partaking in the $[Ru(phen)_3]^{2+}$ P unit) to lie in a coplanar conformation ($\theta^1 \rightarrow 0^\circ$). **1-phen** was shown to exhibit unforeseen improved luminescence while **1-bpy** is almost non-luminescent. Combining photophysical investigations and theoretical modeling allowed us to account for such opposite behavior.

Finally, the derived possibility of switching the emission properties of *P within $[P-(\theta^1)-A]$ via a conformational change is examined.

Results and Discussion

Synthesis: 4-*N*- and 4-*N*-,4'-*N*-(2,4,6-triphenylpyridinio)-substituted 2,2'-bipyridines (**A₁-bpy** and **A₂-bpy**, respectively) are readily obtained by reacting the corresponding amino-bipyridyl derivatives, (NH₂)-bpy and (NH₂)₂-bpy, with commercially available 2,4,6-triphenyl-pyrylium salt. Racemic mixtures of heteroleptic complexes of ruthenium(II) (**0-bpy-4-bpy**; Figure 1) were synthesized according to the standard work-up from [(Me₂bpy)₂RuCl₂] precursor (Me₂bpy is 4,4'-dimethyl-2,2'-bipyridine) and appropriate derivatized bpy ligand. All compounds were fully characterized and their identity was found to comply with expectations.

Solid-state structural features

X-ray analysis: In the solid state, the salient structural features of **1-bpy** (Figure 2a) closely resemble to those of the previously reported H₃TP⁺-substituted ruthenium(II)-bis-terpyridyl analogue, **1-tpy**.^[10b] As expected, the value of θ^1 , 86°, sharply differs from that determined for **1-phen**^[20] of 28° (X-ray crystallography). Other relevant dihedral angles about the pyridinium ring are given in Table 1.

Table 1. Selected dihedral angles (θ°) between the pyridinium ring and its peripheral aryl mean planes (Figure 1) within the acceptor group A of various organic and complex species.

	Ar ^[a]	θ^1	θ^2	θ^6	θ^4
A₁-P ^[b]	ph	77	84	72	20
A₁-P ^[c]	ph	78	72	59	25
A₁-ptpy ^[d]	ph (spacer)	72.60	62.42	65.11	16.45/37.03
A₁-tpy ^[d]	py (tpy)	78.71	55.92	71.18	25.14
A₂-bpy	py (bpy)	75.82	86.70	49.78	33.63
	py (bpy)	73.92	87.50	62.20	44.88
	py (bpy)	82.71	80.06	64.17	38.56
	py (bpy)	77.03	79.62	66.70	42.34
	py (tpy)	79.38	85.48	78.31	24.29
1-tpy ^[d]	py (tpy)	79.38	85.48	78.31	24.29
1-bpy	py (bpy)	86.11	81.78	62.76	40.23
2-bpy	py (bpy)	84.70	89.99	72.17	28.72
	py (bpy)	64.05	58.67	59.48	17.22
P1 A₂/Ru ^[d]	ph (spacer)	87.42	72.85	87.42	46.93
	ph (spacer)	89.21	65.32	73.81	2.13
1-phen ^[e]	"py" (phen)	28	–	–	[f]

[a] *N*-pyridinio aryl substituent; ph: phenyl, py: pyridyl. [b] Ref. [23]. [c] Ref. [24]. [d] Ref. [10b]. [e] Ref. [20]. [f] No data available (ref. [25]).

It was also interesting to determine the X-ray structure of complex **2-bpy** (Figure 2b; Table 1) as the proximity of the two bulky acceptor fragments was predicted to further force them to adopt a canted conformation. Unexpectedly, significantly distinct values of θ^1 were found for the two triarylpyridinium fragments: $\theta^1 = 64.1$ and 84.7° . Thus, apparently, if really conformationally locked, **A₂-bpy** is not the expected *C*₂-symmetrical ligand when complexed. At this stage, it is not clear whether this angular discrepancy of about 20.6° originates from exogenous factors (role of the counteranions among which one is closely tight to one of the pyridinium rings; crystal packing) or to some specific intramolecular constraints related to the rather crowded complex.

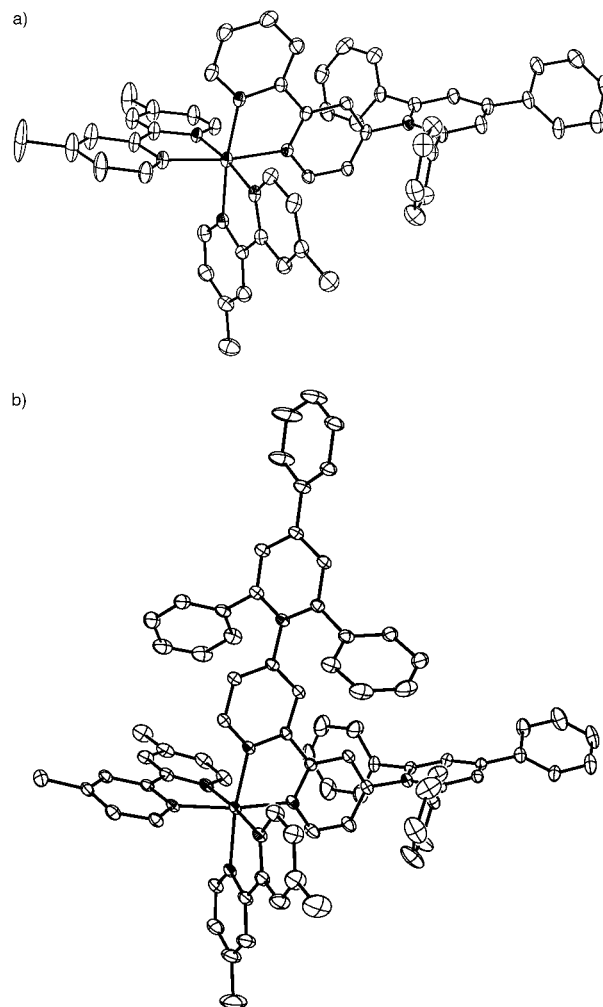


Figure 2. ORTEP drawings of complexes a) [(Me₂bpy)₂Ru(bpy-(tpy₃⁺)₂)]³⁺ (**1-bpy**) and b) [(Me₂bpy)₂Ru(bpy-(tph₃⁺)₂)]³⁺ (**2-bpy**), with thermal ellipsoids (20 and 30% probability, respectively). The hydrogen atoms, PF₆[−] counterions and cocrystallized solvent molecules are omitted for clarity.

The crystal structure of the free organic ligand bearing two acceptor groups (**A₂-bpy**) is shown in Figure 3. The bpy part of the ligands, which is potentially coordinating, is found to adopt the *trans* conformation usually observed in the solid-state for oligopyridyl molecules, with interannular twist angles between pyridyl mean planes of 25.9 and 19.6°.

Within the crystallographic asymmetric unit, each of the two independent molecules exhibits the expected tilted conformation about the acceptor fragment (Figure 3). We have checked that these molecular conformations are truly adopted due to intraligand constraints but not to some interligands effects such as crystal packing (as it is often the case for similar polyaromatic species).^[21] Concerning the values of the critical θ^1 angles, all four vary in a rather narrow range of about 8.8°, compared with the large angular discrepancy above-reported for **2-bpy**.

On the basis of the crystallographic structural data (Table 1), the characteristic values for θ^1 can be estimated

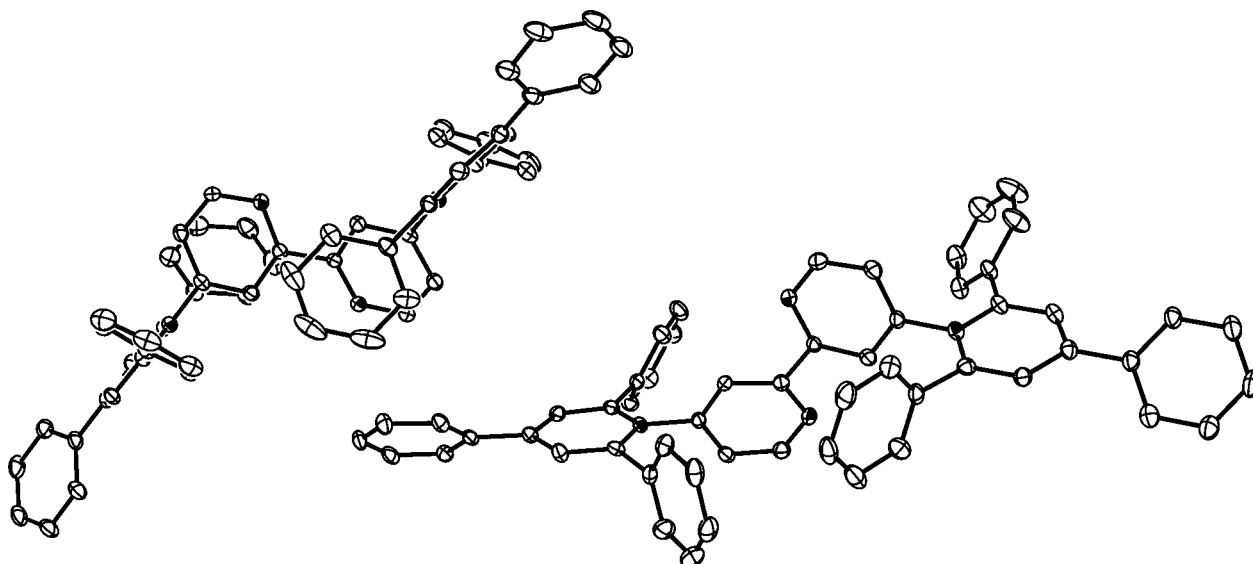


Figure 3. ORTEP drawing of the $(\text{H}_3\text{TP}^+)_2\text{-bpy}$ ligand, **A₂-bpy**, with thermal ellipsoids (30% probability). The hydrogen atoms, BF_4^- counterions and cocrystallized solvent molecules are omitted for clarity.

which actually correspond to an intramolecular compromise between steric repulsion and stabilizing electronic delocalization in the solid-state. Apparently, depending on whether free organic molecules (including ligands) or derivatized complexes are considered, the average value of θ^1 varies from about 77.0 (over eight entries) to 85.4° (over five entries),^[22] respectively. This sizable angular disparity is indicative of different balance between steric and electronic factors in reaction to changes with respect to intramolecular electrostatic repulsion between A (1+) and the initially neutral chromophoric part of derivatized ligands, which gets involved in the positively charged complex photosensitizer (P^{2+}). Also, existing supplementary—steric—interaction within dyads likely to involve the complex photosensitizer (P units) and the bulky substituents of the organic acceptor moiety cannot be excluded (see NMR study).

Solution structural features: Although solid-state investigations such as X-ray analysis provide important quantitative information concerning molecular structures and possible intramolecular constraints, it is worth checking these structural issues against data collected out of solution studies. In the present case, beyond the fact that key photophysical properties of the various dyads will be examined in fluid medium, such a comparison should help in deciding between solid-state specificities and actual intrinsic molecular features of relevance (as for θ^1 angles within **2-bpy**). This study should also provide some insights into intramolecular dynamics, and more particularly the extent of existing restraints (or constraints) over intramolecular motion (e.g. rotation of fragments A).

Chemical behaviour: A striking point stems from the fact that the **A₂-bpy** molecule is merely non-complexing with labile first row transition metal cations such as iron(II). This

behavior further supports the inference of a rather *strong* locking of the molecular conformation in solution, in a fashion similar to that determined in the solid-state (Figure 3). Combined effects of the previously evoked intraligand steric hindrance and electrostatic repulsion between positively charged pyridinium rings might explain this finding. However, these detrimental effects to iron(II) coordination chemistry are not insurmountable for ruthenium(II), which is known to form substantially stronger $\text{Ru-N}(\text{py})$ bonds than iron.^[26]

NMR analysis and structural modelling: In solution, one can reasonably anticipate that, within **1-bpy**, the pyridinium ring remains roughly perpendicular to the attached bpy ligand, as it was shown for the **1-tpy** close structural analogue.^[10b] To confirm the actual conformation of the complexed **A₁-bpy** and **A₂-bpy** ligands, ^1H NMR spectra of the various diamagnetic compounds have been recorded. Combined COSY, TOCSY and NOESY experiments allowed achieving a complete assignment of protons (Figure 4) in spite of the rather complicated features of ^1H NMR spectra.

The C_2 axial symmetry, with C_2 axis bisector of the disubstituted bpy within **2-bpy** (Figure 4), is reflected by the chemical shifts of protons of the four methyl groups of the P unit (Me_2bpy ligands). Indeed, these 12 protons are split into two singlets integrating for six protons in the case of symmetrical **2-bpy** whereas four distinct singlets of three protons are observed in the case of asymmetric compound **1-bpy** (Supporting Information). In the case of **2-bpy**, the recovering of the expected C_2 symmetry in solution as compared to corresponding solid-state findings is indicative of the A groups not conformationally locked but only restrained. Apparently, the degree of freedom for rotation motion is rather large and is at least of about 20° (“floppy torsion”). The broken symmetry observed for the X-ray molecular

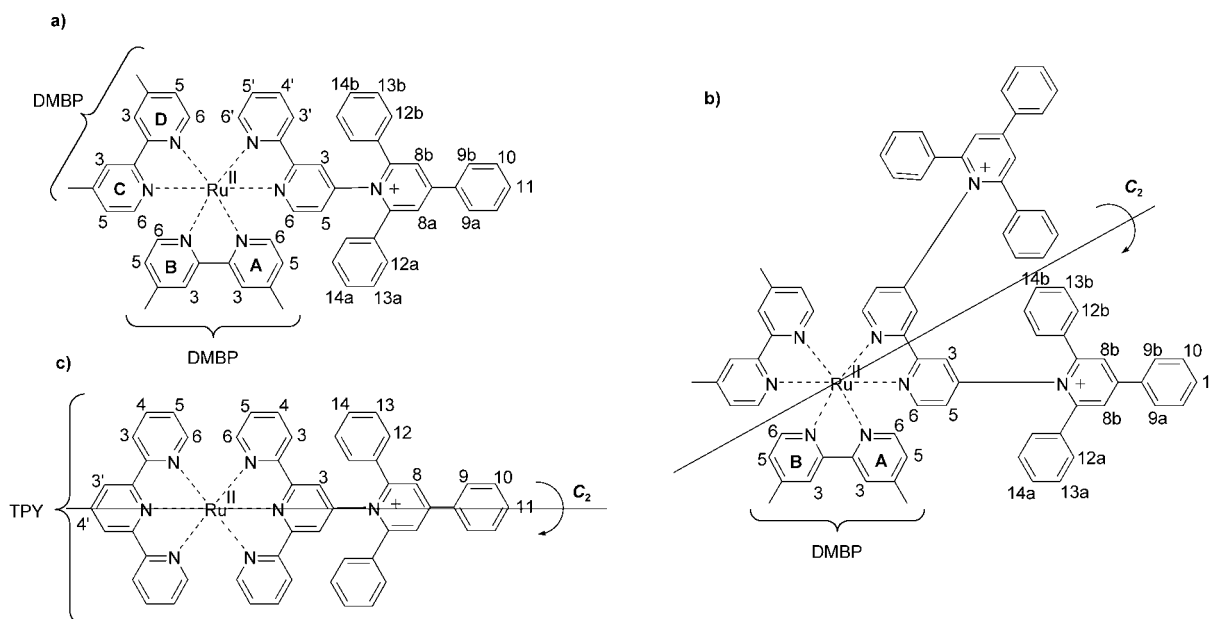


Figure 4. Numbering scheme adopted for ^1H NMR assignments.

structure, displaying two sharply different values of θ^1 , was therefore originating from solid-state specific interactions. Existing degrees of freedom for the rotation motion about θ^1 are further evidenced when performing temperature-dependent NMR studies (cooling mode). Indeed, remarkable changes are observed. However, these modifications are not straightforwardly rationalized as they result from the intermingled effects of the freezing of the various floppy motions of phenyl rings about θ^1 but also θ^2 and θ^6 , which makes it difficult to identify the sole contribution of θ^1 .^[27]

When analyzing the NMR data in more detail, another salient feature is found, which concerns protons H(8). On one hand, these protons appear as a singlet within the free **A₁-bpy** and **A₂-bpy** ligands as well as in complex **1-tpy** (and related **A₁-tpy** free ligand, that is, 4'-(H₃TP⁺)-tpy).^[10b] On the other hand, they are found to be both chemically and magnetically different (and coupled together to give two doublets H8a and H8b) within **1-bpy** and **2-bpy**. The origin of such a differentiation is very likely related to different positioning of protons H(8) with respect to the cones of anisotropy of the canted phenyl rings *ortho* to the $N_{\text{pyridinio}}$ atom(s). Besides, protons of the latter two phenyls (H12, H13 and H14; Figure 4) are also differentiated accordingly (contrary to free ligands and tpy complexes^[10b]). Although these rings are allowed to *slightly* rotate about their respective average tilted positions, the fact that different torsion angles are observed (i.e., $\theta^2 \neq \theta^6$; Figure 1) is probably the indirect consequence of the asymmetric nature (beyond chirality) of the ruthenium(II)-tris-bpy core. The *ortho* phenyl rings appeared undistinguishable (i.e., $\theta^2 \approx \theta^6$) within the C_2 -symmetrical tpy-based reference compound (**1-tpy**). Brought together, these findings further support that involved phenyl groups are neither freely rotating nor completely locked but only restrained. Interestingly, the two sets

(a and b) of protons H8 exhibit almost identical chemical shifts independently of whether mono- or di-substituted complexes **1-bpy** and **2-bpy** are concerned. Thus, inter-acceptors steric hindrance does not explain the canted conformation of groups A rather a P/A intercomponent (including bpy ligands) steric interaction previously inferred from solid-state study.

Concerning the intercomponent decoupling—represented by θ^1 —within **1-bpy**, no proton was found to be adequately positioned to directly probe the local geometry around the P–A linkage (as for **1-tpy**).^[10b] However, based on the above-mentioned similarities of ^1H NMR signals for acceptor groups embedded within **1-bpy** and **2-bpy** together with the factual impossibility for these A groups to deviate too much from perpendicularity within **2-bpy**, one can reason that the actual conformation of A within **1-bpy** is almost orthogonal ($\theta^1 \rightarrow 90^\circ$), as in **1-tpy** (see also Electrochemical Study, below).

After the structural optimization of **2-bpy** starting from the molecular model obtained from the single-crystal X-ray diffraction analysis was computed, a C_2 -symmetrical molecule was indeed obtained. The optimized geometry shows expected features from the ^1H NMR spectra, namely different values for θ^2 and θ^6 (57.84 and 64.32°, respectively) and a unique θ^1 torsion angle of 68.43°. Computed value for θ^1 is smaller than value derived from solid-state data ($\theta^1 \approx 85.4^\circ$). Such a difference, already noticed for other related compounds,^[28] is consistent with above-evidenced floppy torsion.^[27]

Electronic properties: The pivotal question of the actual conformation of P-(θ^1)-A dyads in solution has also been assessed at the electronic level, namely by carrying out a comparative electrochemical study of H₃TP⁺-based dyads (**1-**

bpy and **2-bpy**) with nitro-derivatized analogous complexes (**3-bpy** and **4-bpy**). The choice of NO₂ as a reference substituent was imposed by the facts that i) it is a well-known^[29] π -extending ($-M$ mesomeric effect) and inductive electron-withdrawing ($-I$ effect) group when borne by an aryl fragment^[30] (in other words, NO₂ behaves as a conjugated A-substituent; $\theta^1 \approx 0^\circ$)^[31] and ii) it is expected to have an overall influence on the electronic properties of P similar to that of H₃TP⁺.^[32]

UV/Vis spectroscopy: Ground-state electronic absorption spectra of all new bpy-based compounds and reference species were recorded; the data are given in Table 2.

Table 2. Electronic absorption data and assignments for the [(Me₂bpy)₂Ru(bpyR¹R²)](PF₆)_n complexes in MeCN solutions.

	LC	λ_{max} [nm] ($\epsilon \times 10^4$ [M ⁻¹ cm ⁻¹])	¹ MLCT
0-bpy	207 (7.21), 248 (2.47), 286 (8.36), 323 (1.11)		456 (1.45)
1-bpy	248 (3.79), 286 (8.15), 316 sh (4.95)		433 (1.29), 488 (1.27)
2-bpy	248 sh (5.29), 286 (9.25), 319 (9.82)		421 (1.79), 519 (1.27)
3-bpy	249 (3.07), 284 (6.64)		431 (1.29), 509 (1.32)
4-bpy	248 (3.40), 282 (5.64), 315 (1.94)		428 (1.62), 529 (1.23)

As is the case for tpy analogues,^[10b] the direct attachment of the acceptor to the photosensitizing core results in a sizable perturbation of the electronic properties of the chromophore (Table 2), as illustrated in Figure 5a.

A gradual splitting of the ¹MLCT absorption band situated at 456 nm into two bands is observed in going from **0-bpy** to **1-bpy** and **2-bpy**. Similar changes are also noticed in going from **0-bpy** to **3-bpy** and **4-bpy** as anticipated (Figure 5b). These new bands correspond to MLCT transitions from the metal to the two types of chromophoric ligands, as already reported in the literature for similar heteroleptic compounds.^[15,32]

Electronic transitions of lower energy (MLCT2) participate in the CT to the ligand bearing electron-withdrawing group(s), which is more easily reducible (i.e., derivatized bpy), while the others, at higher energy (MLCT1), involve the π^* orbitals of the more electron-rich ligands (i.e., Me₂bpy). Noteworthy, functionalization of photosensitizers with H₃TP⁺ results in both an increase of molar absorptivities and an extended absorption in the visible region (Figure 5a).^[32,33]

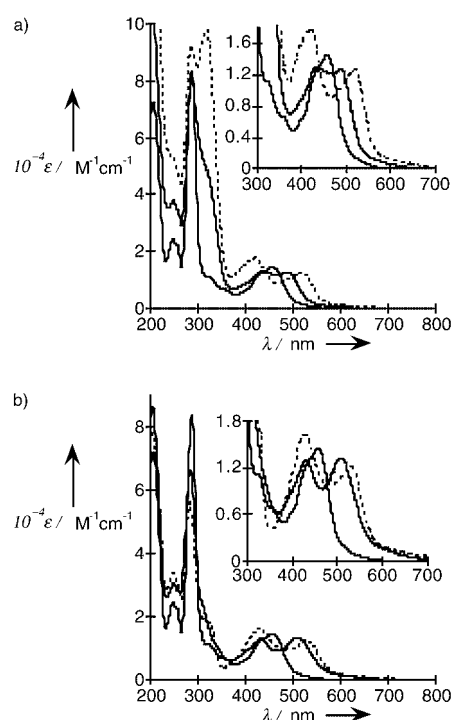


Figure 5. Electronic absorption spectra (room temperature, acetonitrile solution). a) H₃TP⁺ series: **0-bpy** (—), **1-bpy** (---) and **2-bpy** (.....); inset: expanded MLCT region. b) NO₂ series: **0-bpy** (—), **3-bpy** (---) and **4-bpy** (.....); inset: expanded MLCT region.

Electrochemical behaviour: Electrochemical data for reference ligands and related complexes are given in Table 3.

Upon complexation, the redox potential attached to the pyridinium fragments of the functionalized bpy ligands (**A₁-bpy** and **A₂-bpy**), is subject to the same anodic shift of about 0.1 V as the one measured for the related tpy-based compound.^[10a] This finding illustrates the fact that the actual electronic expanse of the acceptor unit involves the *N*-pyridinio substituent (namely the pyridine of the bpy ligand), spreading towards the metal ion. Indeed, the reduction of the pyridinium moiety within **1-bpy** (−0.76 V) is found to

Table 3. Electrochemical data of the examined ligands and related complexes in MeCN (+ 0.1 M NBu₄BF₄) at vitreous carbon electrode.^[a]

	Ru ^{3+/2+} $E_{1/2}$	NO ₂ ^{0/1-} $E_{1/2}$	n	H ₃ TP ^{1+/1-} /PhPy ⁺⁰ $E_{1/2}$	n	P ^{0/1-} $E_{1/2}$	n
A₁-bpy				−0.875	2		
A₂-bpy				−0.881	2 × 2		
0-bpy	+1.19					−1.37	1
1-bpy	+1.28			−0.76	2	−1.47	1
2-bpy	+1.42			−0.76 ^[b]	2 × 2	−1.53	1
3-bpy	+1.29	−0.55	1			−1.12	1
4-bpy	+1.40	−0.48	1			−0.85	1
		−0.63	1				
0-phen^[c]	+1.29					[d]	
1-phen^[c]	+1.42			−0.65 ^[e]	[d]	[d]	

[a] $E_{1/2}$ /V (vs. SCE) is calculated as $(E_{\text{pa}} + E_{\text{pc}})/2$; scan rate 0.2 V s^{−1}; n is the number of electrons involved in the redox process. [b] Average value of potential formally ascribed to the ill-resolved peaks. [c] From ref. [20] $E_{1/2}$ /V (vs. SSCE). [d] No data available. [e] Scan rate 1.0 V s^{−1}.

occur at the same potential (within experimental error) as within **1-tpy** (-0.77 V), as expected for formally identical $[\text{Ru}^{\text{II}}\text{-py-tpy}]^+$ acceptor entities (as defined at the electronic level).

The electrochemical behavior of compounds **0-bpy-4-bpy** (Table 3) parallels the electronic properties, which reflects a certain degree of mutual influence between P and A. H_3TP^+ and NO_2 groups have the same effect upon the $\text{Ru}^{3+/2+}$ metal-centered redox process (anodic shift of the redox potential of ca. 0.1 V per substituent with respect to **0-bpy**), as anticipated.^[15,32] Interestingly, opposite effects are observed upon the $\text{P}^{0/1-}$ ligands-centered redox potential, namely a cathodic shift of about 0.1 V per H_3TP^+ versus an anodic shift of about 0.25 V per NO_2 . Noteworthy, the larger shift is related to the mono-electronic reduction of NO_2 (0.25 V per electron for **3-bpy** and **4-bpy**), whereas the smaller is associated to the bielectronic reduction of H_3TP^+ (ca. 0.05 V per electron for **1-bpy** and **2-bpy**). This difference in sensitivity of the $\text{P}^{0/1-}$ bpy-centered process towards the early reduction of the A groups actually reveals the *distinct* coupling modes of these groups with P. The magnitude of the perturbation is essentially informative on the degree of conjugation ($\pm M \rightarrow 0$) of the A groups with the bpy (and consequently with P). The sign of the shift is more related to the inductive effects of the substituents: A ($-I$) makes the ligand easier to reduce (anodic shift) whereas D ($+I$) makes it more difficult to reduce (cathodic shift).

Based on these findings, it appears that once reduced, the NO_2 substituents remain as the expected conjugated ($-M$) electron acceptors ($-I$), whereas the H_3TP^+ groups behave as electron-rich non-conjugated ($M \rightarrow 0$; $\theta^1 \rightarrow 90^\circ$) and electron-donating ($+I$) units. Thus, the added electron(s) are localized on the H_3TP^+ subunit(s) of the derivatized complexes, which therefore exhibit the behavior of bipartite molecules in solution (despite the above-evidenced noticeable intercomponent electronic coupling). This crucial issue is further supported by the fact that H_3TP^+ is reduced at the same potential regardless of whether or not it is mono- or disubstituted on the same bpy (i.e., **1-bpy** or **2-bpy**), contrary to the NO_2 groups which are communicating via the π -delocalized system of the planar bpy (Figure 6). Noteworthy, in the latter case, the mean value for redox potentials attached to NO_2 groups within **4-bpy** (-0.48 and -0.63 V) that is, -0.55 V corresponds to the reduction potential of the single NO_2 within **3-bpy** (-0.55 V).

To summarize, in addition to valuable thermodynamic characteristics provided, this comparative study further substantiate the statement of persisting geometrical decoupling ($\theta^1 \rightarrow 90^\circ$) for **1-bpy** and **2-bpy** in solution.

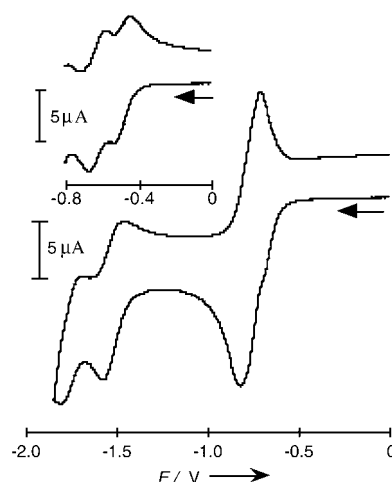


Figure 6. Cyclic voltammogram for **2-bpy**. Inset: selected part of the cyclic voltammogram of **4-bpy** that is, reduction waves attached to the two NO_2 groups.

Photophysical properties: The capability of the new putative compact acceptor dyads (**1-bpy** and **2-bpy**) to undergo intramolecular PET processes has been evaluated by investigating their photophysical behavior (Table 4).

First, it can be noticed, from experimentally derived values of $E(\text{III}/\text{II}^*)$, that the excited-state of P within $^*[\text{1-bpy}]$ is a significantly better reductant (by ca. 0.2 V) than within $^*[\text{1-tpy}]$ (i.e., -0.68 vs -0.51 V, respectively), as expected.

It is also worth noting that the variation of absorption and emission energies as a function of the difference between first oxidation and reduction potentials of complex photosensitizers, ($\Delta E_{1/2} = E_{1/2}(\text{Ru}^{3+/2+}) - E_{1/2}(\text{P}^{0/1-})$), show that MLCT2 absorption correlates like emission features (Figure 7a).^[35] The emitting $^3\text{MLCT}$ state is thus unequivocally the one involving the H_3TP^+ -derivatized bpy ligand (MLCT2), as expected. Disunited correlation of $^1\text{MLCT1}$ and $^1\text{MLCT2}$ absorption bands of both **1-bpy** and **2-bpy** species with respect to emission properties reflects a certain

Table 4. Photophysical data for the H_3TP^+ - and PhPy^+ -derivatized complexes along with the reference-species.^[a]

Entry	298 K					77 K		$E(\text{III}/\text{II}^*)$ [V]
	$\lambda_{\text{max}}^{[\text{b}]}$ [nm]	$\tau^{[\text{c}]}$ [ns]	$\Phi_{\text{em}}^{[\text{d}]}$ [10 ⁻²]	k_{r} [s ⁻¹]	k_{nr} [s ⁻¹]	$\lambda_{\text{max}}^{[\text{b}]}$ [nm]	$\tau^{[\text{c}]}$ [μs]	
0-tpy ^[e]	629	0.56	$\leq 5 \times 10^{-4}$	$\leq 8.9 \times 10^3$	$\geq 1.8 \times 10^9$	598	10.0	-0.76
1-tpy ^[e]	670	55	0.073	1.30×10^4	1.80×10^7	636	8.80	-0.51
0-bpy	625	930	5.73	6.16×10^4	1.01×10^6	588	5.50	-0.92
1-bpy	675	10	0.06	6.00×10^4	9.99×10^7	634	3.88	-0.68
2-bpy	725	108	0.21	1.94×10^4	9.24×10^6	676	1.59	-0.41
0-phen ^[f]	625	510	4.1	8.04×10^4	1.88×10^6	587 ^[g]	^[h]	-0.82
1-phen ^[f]	645	2100	1.0	4.76×10^3	4.71×10^5	605 ^[g]	^[h]	-0.63

[a] Emission properties in deaerated MeCN solutions at 298 K and in deaerated BuCN matrices at 77 K. Radiative (k_{r}) and nonradiative (k_{nr}) rate constants as well as excited-state redox potentials $E(\text{III}/\text{II}^*)$ were calculated according to refs. [15] and [34]. [b] Emission maxima for uncorrected spectra ($\lambda_{\text{exc}} = 460$ nm). [c] $\lambda_{\text{exc}} = 308$ nm unless otherwise specified. [d] Luminescence quantum yields were determined relative to $[\text{Ru}(\text{bpy})_3]^{2+}$ ($\Phi_{\text{em}} = 0.062$ in MeCN at 298 K). [e] From ref. [10a]. [f] From ref. [20]. [g] Estimated value from ref. [20]. [h] No data available.

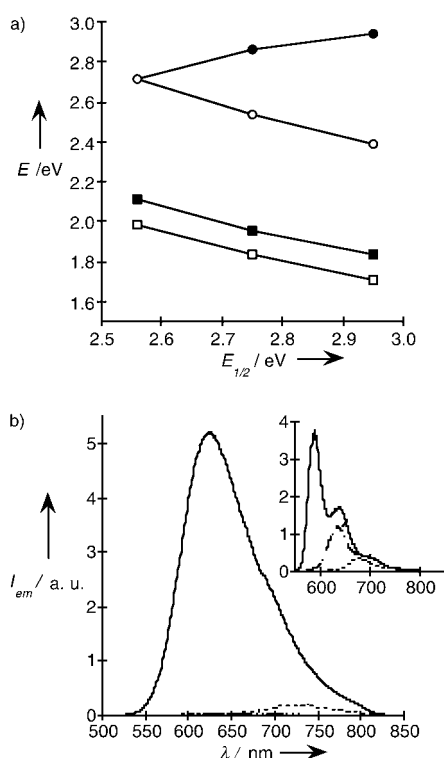


Figure 7. a) Correlation between optical energies (absorption and emission) and ΔE_{vib} (see text), ●: MLCT1, ○: MLCT2, ■: em. (77 K), □: em. (298 K). b) Luminescence spectra of **0-bpy** (—), **1-bpy** (----) and **2-bpy** (.....) (isoabsorptive deoxygenated media, λ_{exc} = 460 nm, uncorrected); MeCN solutions at 298 K. Inset: corresponding uncorrected luminescence spectra in butyronitrile frozen matrix at 77 K.

degree of directionality in the CT state within excited photosensitizer, which should favor rapid electron hopping to A subunit(s) as the lower Ru-bpy CT state (MLCT2) involves the ligand bearing acceptor unit(s).^[36]

At 298 K, the emission quantum yields of **1-bpy** and **2-bpy** are only 1 and 4% of that of parent luminophore **0-bpy**, respectively (Figure 7b). In particular, for **1-bpy**, the radiative decay rate-constant remains almost unchanged while the non-radiative decay is increased by about two orders of magnitude. Clearly, photophysical behavior is distinct at 298 and 77 K (Figure 7b) in spite of equivalent incremental red-shifts (ΔE_{em}) of the emission maxima on going from **0-bpy** to **1-bpy** ($\Delta E_{em}(0-1)$) and **2-bpy** ($\Delta E_{em}(1-2)$) at both temperatures.^[37] The gradual decrease of emission intensity according to bathochromic shift evidenced at 77 K reveals the actual effect of energy gap law. Indeed, only for low-temperature data, a linear relationship could be found when plotting $\ln(1/\tau)$ as a function of $E(^3\text{MLCT})$ (in eV) (slope -4.43 ; intercept 21.34 ; $R=0.95$). Thus, the room-temperature luminescence quenching of *P within **1-bpy** cannot be imputed to sole energy-gap law and a channel which is not operative at 77 K (in rigid matrix, where solvent libration is frozen)—such as an intramolecular PET—must come into play. The status of **2-bpy** at room temperature is discussed below.

Regarding the thermodynamics of **1-bpy**, **2-bpy** and **1-phen**, comparison of ground-state redox potentials of their pyridinium group with corresponding excited-state reductant strength of *P shows that the formation of the CS state is for the whole three an endoergic process by about $+0.08$, $+0.35$ and $+0.02$ eV,^[20] respectively (Figure 8). Although $E(\text{III/II}^*)$ values are roughly estimated,^[15,20,34] the perturbation of *P within **2-bpy** is so large that a CS formation is merely not expected to occur. For **1-bpy** and **1-phen**,^[20] the very slightly unfavorable energetics can be weathered.^[38]

Hence, the luminescence quenching of *P within **1-bpy** can be assigned to an intramolecular PET (Figure 8) all the more since:

- The increase of the ligand field due to electron-withdrawing substituent effect is not expected to influence the emission properties of bpy-based *P, contrary to tpy-based poor luminophores owing to their low lying ^3MC levels (case of **1-tpy**);^[10a,15,20,39,40]
- Energy transfer between *P and *A can be ruled out as the lowest triplet excited-state (phosphorescence at 77 K) of the UV-absorbing H_3TP^+ lies at about 2.5 eV while *P is a NIR-Vis emitter;

A transient absorption experiment at the femtosecond timescale^[41] has not shown clear evidence of the formation of a charge-separated state. As the quenching is slow from energetic considerations while the intercomponent electronic coupling is rather high, this result probably indicates that the charge recombination is much faster than the forward reaction. It is also a matter of fact that the spectral signature of the weakly absorbing reduced acceptor unfortunately falls in the bleaching region of the MLCT bands making it very difficult to detect.^[10b,28] Therefore, together with additional fragility experienced for such complexes in solution, as previously reported for nitro derivatives (analogues of **3-bpy** and **4-bpy**),^[42] the successful completion of photophysical experiments appeared to be very delicate and the detailed quenching mechanism within **1-bpy** could not be definitively established under standard experimental conditions.

Regarding the related case of **1-phen**, quenching of luminescence was not observed, rather the improved emission properties of *P.^[20] This behavior has been ascribed^[20] to the synergetic contributions of the above-mentioned substituent effect and of the small value of θ^1 allowing an electronic delocalization over the entire—and possibly coplanar^[20,38,40] phen-pyridinium ligand, best described as a “superligand”.^[20] It is even likely that planarization of the phen-pyridinium ligand is favored in the excited state, upon its transient photoinduced reduction.^[17d,28,43] This planarization is expected to occur around θ^1 as far as no steric constraint interferes (case of **1-phen**) but also about θ^4 . In the latter case, the conformational change is anticipated to result in an increase of the electron-accepting strength of A,^[17d,44] thus lowering the energy of the CS state—once formed—within *[**1-bpy**] and amplifying the electron delocalization within

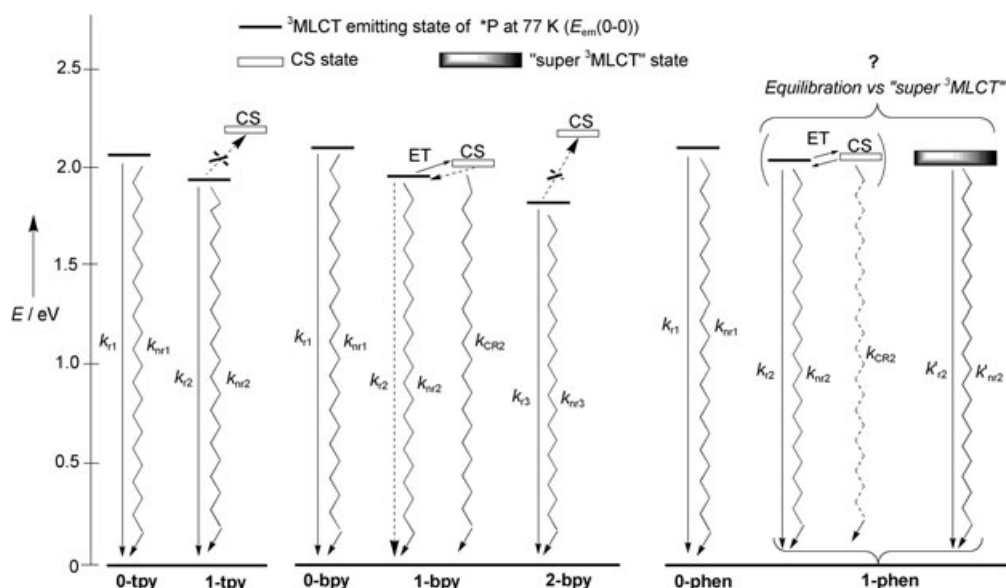


Figure 8. Quantitative energy level diagram for excited states of the series of compounds as well as postulated photoinduced processes. See Table 4 for the relative values of radiative and non-radiative rate constants. Dashed arrows indicate pathways either of low probability or ineffective (see Table 4 and text).

*[**1-phen**]. Whether this electron delocalization actually results from an equilibration process (related to a decay of the CS state to the ground state *via* the closely lying $^3\text{MLCT}$ state) or originates in an intrinsic property of the excited molecule (namely a “super $^3\text{MLCT}$ ” level attached to the phen-pyridinium “superligand”)^[45] remains hitherto unclear (Figure 8).

Theoretical analysis: At this stage of the study, when spectroscopic investigation are reaching the limits of their informative capability, a theoretical analysis of the problem—from first principles—is required. The present aim is to further gain new insights on CS-state formation (case of **1-bpy**) and eventually decide between *dynamic* and *static* electronic delocalization (case of **1-phen**). The computational method herein used is based on density functional theory which has been already demonstrated to accurately account for electronic properties of rather large second and third rows d^6 transition metals complexes.^[28] In particular, the PBE0 hybrid exchange correlation functional was used since it has been proven to give reliable thermochemical and spectroscopic data for similar compounds.^[28,46]

Metal-to-ligand charge transfer electronic transitions can be considered as light-triggered intramolecular redox reaction where the metal center is oxidized while ligands are reduced.^[47] As we are mainly interested in understanding photo-excited states where an electron is promoted on the ligands embedded within complexes, a fruitful approach is to simulate the behavior of mono-reduced species^[28,47] since reduction is known to be essentially a ligand-centered process.^[15] Although singly occupied molecular orbitals (SOMO) usually akin to LUMO orbitals, we preferably fed the discussion on the basis of spin density patterns associated to

SOMOs (rather than SOMO or LUMO orbitals themselves) as the non-negligible contribution of spin polarization originating from inner-lying electrons of the body-molecules are taken into account.^[28] Thus, spin density has been calculated for the following mono-reduced complexes: **1-bpy** for $\theta^1 = 86.11^\circ$ (X-ray structure, [**1-bpy**(86)][−]; Figure 9a) and $\theta^1 = 28^\circ$ (as in **1-phen**, [**1-bpy**(28)][−]; Figure 9b), as well as for **2-bpy** and **1-tpy** (Figure 9c and d) for their geometry determined by X-ray crystallography, that is, [**2-bpy**(64–85)][−] ($\theta^1 = 64.05$ and 84.70°) and [**1-tpy**(79)][−] ($\theta^1 = 79.38^\circ$). Also, spin densities have been computed for incremental values of θ^1 ($0^\circ \leq \theta^1 < 90^\circ$) within [**1-bpy**(θ^1)][−].

The main computational outcomes regarding spin density distributions of the model systems are collected in Table 5.

X-ray data were used for computing the spin density associated to [**1-bpy**][−], [**2-bpy**][−] and [**1-tpy**][−]. As the redox properties attached to the pyridinium ring of A groups are influenced by surrounding substituents^[10a,48] including tilt angles of connected aryl fragments (θ^1 , θ^2 , θ^4 and θ^6),^[17d,20,44] it is therefore worth bearing in mind that slightly different A groups are actually involved in the various complexes although formally identical (H_3TP^+). In the cases of [**1-bpy**(86)][−], [**1-bpy**(28)][−] and [**1-bpy**(θ^1)][−], all structural parameters were kept the same as those determined by X-ray crystallography of **1-bpy**(86) except θ^1 dihedral angle. This was done on purpose, to clearly and solely identify the contribution of critical θ^1 twist angle to the electronic and photophysical properties of *[**0-bpy**] (i.e., *P).

Also, one can notice the lack of symmetry of the overall—actual—**1-tpy**(79) molecule (frozen in its solid-state conformation) mainly originating from different values for θ^2 , θ^4 and θ^6 torsion angles, as in the case of **1-bpy**(86). As a consequence, similar asymmetrical distributions of spin

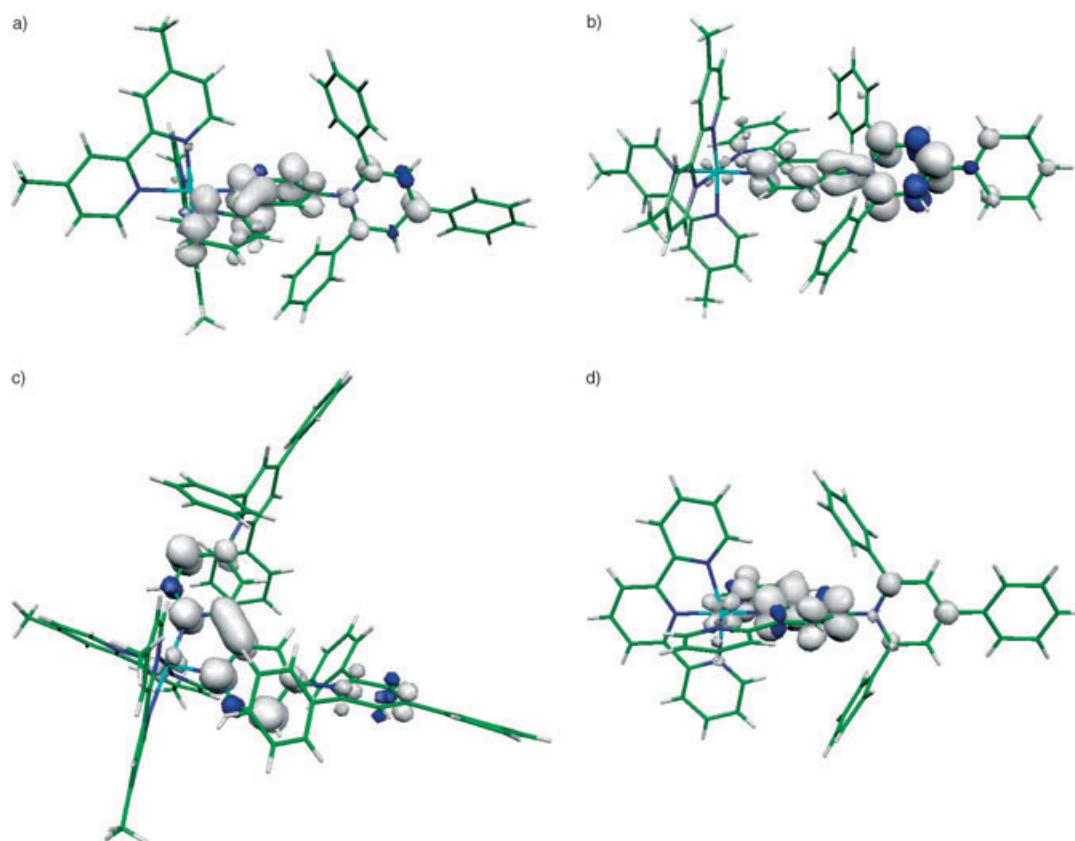


Figure 9. Computed spin densities (contour value 0.0025 au) for a) $[1\text{-bpy}(86)]^-$, b) $[1\text{-bpy}(28)]^-$, c) $[2\text{-bpy}(64\text{--}85)]^-$ and d) $[1\text{-tpy}(79)]^-$.

Table 5. Computed spin density (in a.u.) for the following mono-reduced complexes: for $[1\text{-bpy}(86)]^-$, $[1\text{-bpy}(28)]^-$, $[1\text{-bpy}(\theta^1)]^-$, $[2\text{-bpy}(64\text{--}85)]^-$ and $[1\text{-tpy}(79)]^-$.

Entry	Ru	L–A	L	A	pyridinium	aL
$[1\text{-tpy}(79)]^-$	0.049	0.945	0.816	0.129	0.107	0.007
$[1\text{-bpy}(86)]^-$	0.010	0.881	0.731	0.150	0.140	0.043/0.085
$[1\text{-bpy}(75)]^-$	0.010	0.904	0.667	0.238	0.226	0.039/0.057
$[1\text{-bpy}(60)]^-$	0.009	0.943	0.630	0.312	0.303	0.017/0.031
$[1\text{-bpy}(45)]^-$	0.018	0.951	0.518	0.433	0.418	0.009/0.021
$[1\text{-bpy}(28)]^-$	0.020	0.959	0.452	0.507	0.487	0.006/0.014
$[1\text{-bpy}(15)]^-$	0.019	0.964	0.405	0.562	0.531	0.004/0.009
$[1\text{-bpy}(0)]^-$	0.023	0.965	0.383	0.581	0.539	0.003/0.007
$[2\text{-bpy}(64\text{--}85)]^-$	0.030	0.951	0.880	0.058–0.013	0.056–0.005	0.006/0.010

L–A: A-derivatized ligand ($A_{1/2}$ -bpy or A-tpy). L: coordinating part of L–A (i.e., bpy or tpy). A: 2,4,6-triphenylpyridinium, H_3TP^+ . aL: ancillary ligand(s) (Me_2 -bpy or tpy).

density were found on the chromophoric part of derivatized ligands within $[1\text{-tpy}(79)]^-$ (Figure 9d) and $[1\text{-bpy}(86)]^-$ (Figure 9a).

Comparison of 1-tpy and 1-bpy: On going from $[1\text{-tpy}(79)]^-$ to $[1\text{-bpy}(86)]^-$, a sizable decrease of spin density located on the ruthenium is noticed, which parallels the decrease of the redox potential related to the one-electron oxidation process of the metal center: from +1.44 to +1.28 V (vs SCE), respectively. The same trend is found on going from $[2\text{-bpy}(64\text{--}85)]^-$ ($E_{1/2}(\text{Ru}^{\text{III/II}}) = +1.42$ V) to $[1\text{-bpy}(28)]^-$ and $[1\text{-bpy}(86)]^-$ ($E_{1/2}(\text{Ru}^{\text{III/II}}) = +1.28$ V), thus allowing estimating

$E_{1/2}(\text{Ru}^{\text{III/II}})$ the redox potential of Ru within hypothetical $[1\text{-bpy}(28)]^-$ of intermediate metal-centered spin density (Table 5) as being of about +1.35 V. This is in line with above-mentioned influence of conjugation over the pyridinium redox properties that is, the pyridinium is a slightly better electron-acceptor group when $\theta^1 = 28^\circ$ than when θ^1 tends toward 90° ,^[17d, 44] making the metal cation more difficult to oxidize. Although non-negligi-

ble, the magnitude of the latter effect remains modest.

Notably, when going from $[1\text{-tpy}(79)]^-$ to $[1\text{-bpy}(86)]^-$, significantly less spin density is located on L–A ligand and geometrical features regarding π conjugation are getting less favorable (θ^1 varies from 79 to 86°). Yet, the net spin density located on A, and more specifically on the pyridinium ring, is substantially increased by about 30%. Such a change is in agreement with our expectations and further supports the pertinence of replacing the $^*[\text{Ru}(\text{tpy})_2]^{2+}$ light-triggered primary donor by the $^*[\text{Ru}(\text{bpy})_3]^{2+}$ analogue for CS purposes.

Comparison of 1-bpy(86) and 1-bpy(28)/1-phen(28): On going from $[1\text{-bpy}(86)]^-$ to $[1\text{-bpy}(28)]^-$, the spin density originally mainly located on the bpy moiety, L, of the $A_1\text{-bpy}$ ligand, L–A (proportions of ca. 5:1 for L:A), becomes almost equally distributed over the whole $A_1\text{-bpy}$ ligand. The sole but moderate increase of the electron-withdrawing strength of the pyridinium ring, according to the previously discussed π conjugation with the bpy, cannot account for such a *large* change of electron distribution. When plotting relative spin densities calculated for $[1\text{-bpy}(\theta^1)]^-$ as a function of θ^1 (Figure 10), almost the same distribution pattern

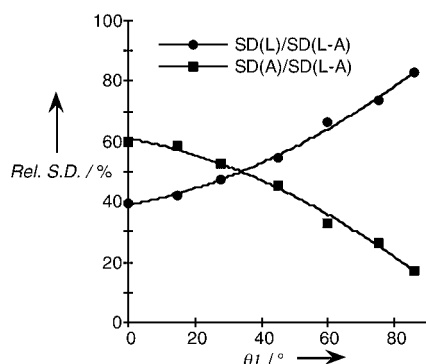


Figure 10. Variation of the relative spin density (SD) distributions over A and L moieties of L–A embedded within $[1\text{-bpy}(\theta^1)]^-$ as a function of θ^1 . Spin densities are normalized with respect to the corresponding total spin density calculated for L–A.

as in $[1\text{-bpy}(28)]^-$ is obtained for θ^1 ranging from 0 to $\approx 35^\circ$. Moreover, in this range, roughly the same spin density is shared out evenly over the six non-hydrogen atoms of both the pyridinium ring and its attached pyridyl fragment of bpy (Figure 9b and Table 5). The quasi-independence of the spin density distribution from θ^1 angle together with its uniformity is indicative of intrinsic electron delocalization. These findings allow to rule out the occurrence of an intramolecular dynamic equilibration process between two closely lying levels like $[^3\text{P}^*\text{-A}]$ and $[\text{P}^+\text{-A}^-]$,^[49] which may exist for higher values of θ^1 , around 40 to 50° .

Although taking place at the excited state, the distinction between *static* (intrinsic) and *dynamic* electron delocalization is somehow reminiscent of that established by Robin and Day for direct optical ET within inorganic mixed-valence species.^[50] Indeed, electronic properties of mixed-valence compounds are accurately accounted by the so-called Class III or Class II models depending on whether electron delocalization: i) is an intrinsic property (i.e., delocalized ground-state) likened here to a “super- $^3\text{MLCT}$ ” state ($[^3\text{P}^*\text{-A}]$ and $[\text{P}^+\text{-A}^-]$ states are merged together) or ii) is thermally activated (i.e., results from an electron transfer) similarly to an equilibration process, respectively.^[51]

When θ^1 approaches 90° , the contribution of the conjugation vanishes making the spin density localized, with different weights on the L and A moieties. Although predomi-

nantly located on the bpy moiety (Figures 9a and 10), the substantial spin density found on the H_3TP^+ fragment further confirms the possibility of an electron transfer from excited complex photosensitizer ($[^3\text{P}^*\text{-A}]$ that is, $^3\text{MLCT}$ state) to the acceptor ($[\text{P}^+\text{-A}^-]$ CS state) within $[1\text{-bpy}(86)]^-$ (Figure 8).

For $[1\text{-bpy}(28)]^-$, one is actually dealing with an electronic delocalization, which is an *intrinsic* property of the $A_1\text{-bpy}(28)$ ligand worth to be considered as a made-in-one-piece “superligand” rather than a bipartite molecule, as in the case of $A_1\text{-bpy}(86)$. The effect of the delocalization over the superligand is to minimize the average local structural distortion related to the presence of the promoted electron, making Franck-Condon factors smaller and then diminishing the rate of nonradiative decay.^[45] Improved emission properties of $[1\text{-phen}(28)]^-$ (and more specifically excited-state lifetime) are therefore worth describing as originating from a “super- $^3\text{MLCT}$ ” level (Figure 8).

The overall picture drawn out of the theoretical comparative study of hypothetical $[1\text{-bpy}(28)]^-$ (mimicking $[1\text{-phen}]^-$) with existing $[1\text{-bpy}(86)]^-$ is in agreement with issues based on the cross photophysical results of the present and previous^[20,38] works. Also, this study allows to clarify the behavior of $[1\text{-phen}]^-$ in respect of electronic delocalization versus equilibration process (Figure 8). Theoretical issues clearly show that photophysical behavior of $[1\text{-phen}]^-$ is consistent with a *delocalized* description associated to an emitting extended “super- $^3\text{MLCT}$ ” level, as illustrated by $[1\text{-bpy}(28)]^-$ model compound. Conversely, a *localized* description well accounts for the behavior evinced by $[1\text{-bpy}(86)]^-$, further substantiating the possibility of a PET process accompanied by CS formation.

Thus, one can state that in the borderline case of isoenergetic $[^3\text{P}^*\text{-A}]$ and $[\text{P}^+\text{-A}^-]$ excited-states within a potentially fully conjugated molecule of type P-(θ^1)-A, occurrence of an intramolecular PET process (accompanied with CS formation) is strongly dependent on a conformational parameter (θ^1). Consequently, other potentially interesting related photophysical features such as luminescence can also be controlled by θ^1 .^[52]

Comparison of 2-bpy(64–85) and 1-bpy(86)/1-tpy(79): Interestingly, when comparing $[1\text{-bpy}(86)]^-$ to $[2\text{-bpy}(64\text{–}85)]^-$, one can note that in spite of a sizable increase of the spin density on L–A (by ca. 10 %), the cumulated spin density on the two A groups dramatically decreases by about 53 %. More strikingly, when comparing the spin density on A within $[1\text{-bpy}(86)]^-$ with the one located on the A group of $[2\text{-bpy}(64\text{–}85)]^-$ with almost the same θ^1 angle (85°), the decrease is about one order of magnitude. The absolute spin density located on the acceptor groups represents no more than about 7.5 % of the overall spin density located on L–A (0.951 a.u.), which sharply differs from the situation of $[1\text{-bpy}(86)]^-$ where this proportion reaches about 17.5 % (over 0.851 a.u.) moreover with a single acceptor unit.

Furthermore, spin density patterns on the L–A ligand within $[1\text{-tpy}(79)]^-$ and $[2\text{-bpy}(64\text{–}85)]^-$ are very similar,

thus suggesting that the poor luminescence properties of *P within $^*[2\text{-bpy}]$ are very likely due to strong substituent effects exerted by the two acceptor groups and are well accounted by energy gap law. The main difference between these two species stems from the fact that, in the case of **2-bpy**, there is no unfavorable interplay between the intrinsically poorly emissive $^3\text{MLCT}$ state (due to energy gap law) and a closely lying non-radiative deactivation pathway ligand field in nature, as for **1-tpy**. Indeed, in the latter case, the removal of this ^3MC state due to the inductive through σ bond (P–A linkage) mediated electron-withdrawing effect did result in improved photophysical properties despite energy gap law.

General comments: We have shown that a strong intramolecular electronic coupling is not incompatible with occurrence of PET processes eventually resulting in CS-state formation. To some extent, this behavior is reminiscent of the function of a photoactive molecular wire.^[8c,e,53] For electron molecular wires such as symmetrical mixed-valence complexes,^[54] the initial (ground) state is different from the final (ground) one, hence the notion of transfer. In the present case, the final state is the same as the initial one (the unique ground state) and the concept of transfer is valid for the excited state only. Such an operation is therefore closely linked to a *localized* description of photo-triggered phenomena. Electron transfer proceeds according to a stepwise manner by hopping from one localized excited state to another. In that sense, by undergoing a *directional* PET process, **1-bpy** constitutes an improvement as compared to both **1-tpy**^[10a] and **1-phen**.^[20] In the latter case, worth described with a *delocalized* model, no such transfer nor CS formation occurs.^[20] It remains nonetheless that, when formed, the CS state is very short-lived due to the *strong* intramolecular electronic coupling (case of **1-bpy**). On the basis of issues herein reported, in a further step, efforts should therefore be directed toward slowing down CR while speeding up the forward ET (CS formation), which should be achieved by making the CS formation significantly exergonic. Such a challenging objective is realistic even with *compact* covalent assemblies, without any spacer element as such, and at least when intramolecular electronic coupling is weak. A famous and quite unique illustration concerns $\text{Ru}^{\text{II}}/\text{Os}^{\text{II}}$ complexes of polycyclic aromatic dppz (dipyrido[3,2-*a*:2',3'-*c*]phenazine) and related ligands, including bridging derivatives. These planar fully conjugated and structurally made-in-one-piece species actually exhibit electronic properties of bipartite molecules comprising a chromophoric phen subunit (part of P) and a phenazine-like electron-acceptor unit (A) in the typical case of dppz.^[55–59] Within one of these systems, a long-lived CS state of about 1.3 μs could be obtained.^[16] Also, very recently, Fukuzumi and co-workers^[60] succeeded in reaching hundreds of μs timescale for CS lifetimes within a dyad based on weakly coupled Zn-porphyrin (P/D) and C_{60} (A) as well as in a purely organic bipartite molecule build up of mesityl (P/D) and methyl-acridinium (A) moieties. However, in spite of these recent advances towards ultra

long-lived CS states, still the very detailed working mode of these compact dyads has to be elucidate.^[61]

The promising “compact approach” requires at one and the same time a particularly fine-tuning of electronic properties and a precise control of intramolecular geometry to slow down backward ET (charge recombination). It's a matter of fact that, on one hand, $\text{Ru}^{\text{II}}/\text{Os}^{\text{II}}$ oligopyridyl complexes are very well documented from viewpoint of MLCT manipulation and, on the other hand, triarylpyridinium electron-acceptor units reveal chemical versatility, which allows both structural and electronic engineering. Therefore, we are currently continuing our effort in the conception of compact architectures, in parallel with more conventional approach to long-lived CS-state formation based on long-range ET within nanosize redox cascades.^[10,28] Also, the study of such molecular objects should help in identifying actual determining parameters that govern slow charge recombination, beyond classical guidelines of well-established ET theory.^[61,62]

Another aspect of the present work that deserves to be emphasized is the advantage that could be taken of the marked sensitivity of photophysical properties displayed by particular assemblies herein studied to changes of intramolecular conformation (θ^1). This strong dependence is ascribed to the combined effects of the compact arrangement of P and A units (that allows the resulting P-(θ^1)-A dyad to be fully conjugated) and of the closely lying (even isoenergetic) [$^3\text{P}^+-\text{A}$] (i.e., $^3\text{MLCT}$ level) and [P^+-A^-] (i.e., CS state) potential excited states. Depending on whether θ^1 approaches 90 or 0°, [$^3\text{P}^+-\text{A}$] and then [P^+-A^-] states or a single “super- $^3\text{MLCT}$ ” state (from formally merged [$^3\text{P}^+-\text{A}$] and [P^+-A^-] levels) are produced upon light-excitation of P within P-(θ^1)-A. In the former case, a side effect of CS formation is the concomitant quenching of the luminescence of *P .^[63] Thus, it appears that the emission properties of P within P-(θ^1)-A type of supermolecules can be conformationally switched. Attempts towards switching effects with respect to electron transport, similarly produced on the sole basis of conformational changes within electron wires, were not entirely successful. As a matter of facts, electron transfer/transport processes are not sensitive enough to this type of parameter,^[17e,18b,18c,19a] contrary to luminescence^[52] under proper conditions mentioned above.^[64] A possible application of such switching effects could be for an optical information storage at the molecular level based on the luminescence of *P .^[65] Also, the derived possibility of a conformational tuning of nonlinear two-photon absorption processes^[66] that could be use for molecule-based photonic materials should be investigated inasmuch the type of compounds studied are also known to exhibit NLO properties.^[67,68]

Conclusion

The localized description of a *dyad system* moreover capable of undergoing an *intercomponent*, that is, a directional PET process, fruitfully accounts for the photophysical behavior of

*[1-bpy] despite the strong intramolecular electronic coupling. On the contrary, *[1-phen] is worth considered as being a “large molecule” (versus “supramolecular species”)^[8c] best described in terms of excited-state electron delocalization over the phen-pyridinium superligand with enhanced emission properties shown to originate from corresponding “super-³MLCT” level. Also, it is demonstrated here, by comparing the borderline cases of these closely affiliated complexes, that the emission properties of *P can be conformationally switched by changing the dihedral angle ($0^\circ \leftarrow \theta \rightarrow 90^\circ$) between the chromophoric part of a ligand (bpy) and its directly connected electron-accepting moiety within the compact P-(θ)-A supermolecule (e.g. *[1-bpy(θ)]).

Experimental Section

General experimental details: Electronic absorption spectra were measured on a Perkin–Elmer Lambda 9 spectrophotometer. ¹H NMR spectra were recorded on a Bruker ARX 250 spectrometer. For inorganic compounds (racemic heteroleptic complexes), unless otherwise specified (i.e., label DMBP stands for Me₂bpy ancillary ligands), ¹H assignments refer to the derivatized bpy ligands (4-nitro-bpy, 4,4'-dinitro-bpy, **A₁-bpy**, **A₂-bpy**, including native bpy). Elemental analyses were performed at the Institut de Chimie des Substances Naturelles, France. ESI(+) mass spectra (solvent, acetonitrile) were recorded with a LCQ-advantage (ThermoFinnigan) mass spectrometer.

Chemicals: High-purity commercial reagent grade products were used without further purification, including the ligands bpy and Me₂bpy (DMBP), which were obtained from Aldrich Chemicals Co. Ltd. Ligands NO₂-bpy,^[69,70a] (NO₂)₂-bpy^[70] and organic precursors NH₂-bpy^[71,72] and (NH₂)₂-bpy^[72] as well as the complex precursor [(dmbp)₂RuCl₂]^[73] were synthesized following the literature methods.

Ligand [H₃TP⁺-bpy](HSO₄) (A₁-bpy**):** The ligand was prepared by following a modification of the literature method for the synthesis of **H₃TP⁺-tpy** analogue.^[10b] A mixture of NH₂-bpy (0.19 g, 1.11 mmol), 2,4,6-triphenylpyrylium hydrogen sulfate (0.677 g, 1.66 mmol, 1.5 equiv) and anhydrous sodium acetate (1.0 g) in EtOH (20 mL) was heated under reflux for 16 h. After evaporation of the solvent in a Rotavapor, the product was extracted from the solid with CH₂Cl₂ and purified by column chromatography over basic alumina by using a mixture of eluents with an increasing gradient of polarity: EtOAc/CH₂Cl₂ 100:0 → 0:100 and then CH₂Cl₂/EtOH 99:1 → 50:50. The pure product was obtained as a white solid (0.352 g, 55.8%). ¹H NMR (250 MHz, CD₃CN): δ = 8.60 (brd, ³J = 4.0 Hz, 1H; H^{3b}), 8.50 (d, ³J = 5.4 Hz, 1H; H⁶), 8.48 (s, 2H; H⁸), 8.36 (d, ⁴J = 1.9 Hz, 1H; H³), 8.28 (d, ³J = 8.0 Hz, 1H; H⁶), 8.15 (dd, ³J = 7.7, ⁴J = 1.8 Hz, 2H; H⁵), 7.87 (td, ³J(H⁵H⁶) ≈ ³J(H⁵H⁴) = 7.8, ⁴J(H⁵H³) = 1.7 Hz, 1H; H⁵), 7.72 (m, 3H; H¹⁰, H¹¹), 7.44 (m, 11H; H¹², H¹³, H¹⁴, H⁴), 7.35 ppm (dd, ³J = 5.3, ⁴J = 1.9 Hz, 1H; H⁵); elemental analysis (%) calcd for C₃₃H₂₅N₃SO₄·0.5H₂O: C 69.70, H 4.61, N 7.39; found: C 69.95, H 4.60, N 7.03; ES-MS: *m/z*: 462.3 [M–HSO₄]⁺.

Ligand [(H₃TP⁺)₂-bpy](BF₄)₂ (A₂-bpy**):** The procedure was similar to that described for **A₁-bpy**, by using (NH₂)₂-bpy (0.158 g, 0.85 mmol), 2,4,6-triphenylpyrylium tetrafluoroborate (1.010 g, 2.55 mmol, 3 equiv) and anhydrous sodium acetate (1.0 g) in EtOH (30 mL) heated to reflux for 20 h. At room temperature, the white precipitate was filtered off and washed with EtOH (2 × 10 mL). The product was extracted from the solid with CH₂Cl₂ (4 × 50 mL), and the solvent was evaporated, affording pure **A₂-bpy** ligand as white needles (0.645 g, 79%). ¹H NMR (250 MHz, CD₃CN): δ = 8.46 (s, 4H; H⁸), 8.41 (d, ³J = 5.2 Hz, 2H; H⁶), 8.14 (m, 6H; H⁹, H³), 7.72 (m, 6H; H¹⁰, H¹¹), 7.40 (m, 22H; H¹², H¹³, H¹⁴, H⁵); elemental analysis (%) calcd for C₅₆H₄₀N₄B₂F₈·H₂O: C 70.02, H 4.41, N 5.83; found: C 69.94, H 4.53, N 5.53; ES-MS: *m/z*: 855.3 [M–BF₄]⁺.

Complex [(dmbp)₂Ru(bpy)](PF₆)₂ (0-bpy**):** bpy (0.243 g, 1.56 mmol, 1.2 equiv) and 1,2-ethanediol (40 mL) were added to a solution of [(dmbp)₂RuCl₂] (0.7 g, 1.295 mmol) in CH₂Cl₂ (20 mL), and the mixture was heated at 110 °C for 20 h under inert atmosphere (Ar). After the mixture had cooled, EtOH (10 mL), H₂O (40 mL) were added together with an excess of NH₄PF₆ salt (2.11 g, 12.95 mmol, 10 equiv/Ru), while vigorously stirring, for the precipitation of the complex. The product was filtered off, washed successively with H₂O, EtOH, and Et₂O, to give an orange powder which was purified by column chromatography over basic alumina by using an eluent of increasing polarity: CH₂Cl₂/acetone 100:0 → 0:100. The final recrystallization was performed by slow diffusion of Et₂O in a concentrated acetonitrile solution of the complex, affording **0-bpy** as deep orange crystals (1.04 g, 86%). The racemic mixture ($\Lambda + \Delta$) was not resolved. ¹H NMR (250 MHz, CD₃CN): δ = 8.48 (d, ³J(H³H⁴) = 8.2 Hz, 2H; H³), 8.35 (s, 4H; H^{3,DMBP}), 8.04 (td, ³J(H⁴H³) ≈ ³J(H⁴H⁵) = 8.1, ⁴J(H⁴H⁶) = 1.1 Hz, 2H; H⁴), 7.74 (d, ³J(H⁶H⁵) = 5.4 Hz, 2H; H⁶), 7.54 (d, ³J(H^{6,DMBP}H^{5,DMBP}) = 5.7 Hz, 2H; H^{6,DMBP}) + 7.53 (d, ³J(H^{6,DMBP}H^{5,DMBP}) = 5.7 Hz, 2H; H^{6,DMBP}), 7.39 (t, ³J(H⁵H⁶) ≈ ³J(H⁵H⁴) = 6.6 Hz, 2H; H⁵), 7.23 (d + d, ³J(H^{5,DMBP}H^{6,DMBP}) ≈ 5.0 Hz, 2H + 2H; H^{5,DMBP}), 2.54 ppm (s, 12H; H^{Me,DMBP}); elemental analysis (%) calcd for C₃₄H₃₂N₄RuP₂F₁₂·H₂O: C 43.74, H 3.67, N 9.00; found: C 43.89, H 3.66, N 9.05; ES-MS: *m/z*: 771.1 [M–PF₆]⁺, 313.2 [M–2PF₆]²⁺.

Complex [(dmbp)₂Ru(bpy-tpb⁺)](PF₆)₃ (1-bpy**):** A procedure similar to that reported for **0-bpy** was followed, by using [(dmbp)₂RuCl₂] (0.159 g, 0.295 mmol) dissolved in CH₂Cl₂ (4 mL), [H₃TP⁺-bpy](HSO₄)·0.5H₂O (0.201 g, 0.354 mmol, 1.2 equiv) and 1,2-ethanediol (40 mL). The mixture was heated at 110 °C for 20 h under Ar. After standard work-up for purification including metathesis, the product was subsequently purified by column chromatography over basic alumina, first eluting with CH₂Cl₂/acetone using a gradient of acetone (up to 100%), second with CH₃CN and finally with a saturated CH₃CN solution of NH₄PF₆. After removal of the salt in excess, the product was four times recrystallized by slow vapor diffusion of Et₂O in a solution of the complex in acetone. The final crystallization was performed by slow diffusion of Et₂O in a concentrated acetonitrile solution of the complex, giving dark red crystals (0.189 g, 46.3%). The racemic mixture ($\Lambda + \Delta$) was not resolved. ¹H NMR (250 MHz, CD₃CN): δ = 8.58 (d, ⁴J(H^{8b}H^{8a}) = 1.9 Hz, 1H; H^{8b}), 8.53 (d, ⁴J(H^{8a}H^{8b}) = 2.0 Hz, 1H; H^{8a}), 8.35 (brs, 2H; H^{3,DMBP}, H^{3D,DMBP}), 8.31 (brs, 1H; H^{3A,DMBP}), 8.30 (brs, 1H; H^{3B,DMBP}), 8.19 (m, 3H; H^{9a}, H³, H^{9b}), 8.04 (m, 2H; H³, H⁴), 7.74 (m, 3H; H¹⁰, H¹¹), 7.66 (d, ³J(H⁶H⁵) = 5.5 Hz, 1H; H⁶), 7.57 (m, 7H; H^{6,DMBP}, H^{14b}, H^{13b}, H^{12b}, H⁶), 7.41 (t, ³J(H⁵H⁴) ≈ ³J(H⁵H⁶) = 5.6 Hz, 1H; H⁵), 7.36 (d, ³J(H^{6B,DMBP}H^{5B,DMBP}) = 6.0 Hz, 1H; H^{6B,DMBP}), 7.24 (m, 8H; H^{5D,DMBP}, H^{5A,DMBP}, H^{14a}, H^{12a}, H^{5C,DMBP}, H^{6A,DMBP}, H^{5B,DMBP}), 7.08 (m, 3H; H⁵, H^{13a}), 6.97 (d, ³J(H^{6D,DMBP}H^{5D,DMBP}) = 5.8 Hz, 1H; H^{6D,DMBP}), 2.65 (s, 3H; H^{MeA,DMBP}), 2.58 (s, 3H; H^{MeD,DMBP}), 2.54 (s, 3H; H^{MeC,DMBP}), 2.51 ppm (s, 3H; H^{MeB,DMBP}); elemental analysis (%) calcd for C₃₇H₄₈N₇RuP₃F₁₈·H₂O: C 49.43, H 3.64, N 7.08; found: C 49.66, H 3.68, N 7.09; ES-MS: *m/z*: 1222.2 [M–PF₆]⁺, 538.6 [M–2PF₆]²⁺, 310.9 [M–3PF₆]³⁺.

Complex [(dmbp)₂Ru(bpy-(tpb⁺)₂)](PF₆)₄ (2-bpy**):** The synthetic method is the same as the one reported for **1-bpy**, using [(dmbp)₂RuCl₂] (0.18 g, 0.333 mmol) in CH₂Cl₂ (4 mL) and [(H₃TP⁺)₂-bpy](BF₄)₂·H₂O (0.384 g, 0.4 mmol, 1.2 equiv) in CHCl₃ (10 mL) to give the pure **2-bpy** compound as dark brown crystals (0.163 g, 26.4%). The racemic mixture ($\Lambda + \Delta$) was not resolved. ¹H NMR (250 MHz, CD₃CN): δ = 8.60 (d, ⁴J(H^{8b}H^{8a}) = 1.9 Hz, 2H; H^{8b}), 8.55 (d, ⁴J(H^{8a}H^{8b}) = 1.9 Hz, 2H; H^{8a}), 8.32 (brs, 4H; H^{3A,DMBP}, H^{3B,DMBP}), 8.17 (d, ³J(H^{9(a+b)}H¹⁰) = 6.8 Hz, 4H; H^{9a}, H^{9b}), 7.75 (m, 10H; H¹⁰, H¹¹, H³, H^{14b}), 7.59–7.42 (m, 12H; H^{13b}, H^{12b}, H⁶, H^{6B,DMBP}), 7.31 (m, 4H; H^{5A,DMBP}, H^{14a}), 7.20 (brd, 8H; H^{12a}, H⁵, H^{5B,DMBP}), 7.11 (t, ³J(H^{13a}H^{12a}) ≈ ³J(H^{13a}H^{14a}) = 7.6 Hz, 4H; H^{13a}), 6.58 (d, ³J(H^{6A,DMBP}H^{5A,DMBP}) = 5.8 Hz, 2H; H^{6A,DMBP}), 2.71 (s, 6H; H^{MeA,DMBP}), 2.52 ppm (s, 6H; H^{MeB,DMBP}); elemental analysis (%) calcd for C₈₀H₆₄N₈RuP₄F₂₄·2H₂O: C 51.82, H 3.70, N 6.04; found: C 51.74, H 3.66, N 6.01; ES-MS: *m/z*: 1673.1 [M–PF₆]⁺, 764.1 [M–2PF₆]²⁺, 461.1 [M–3PF₆]³⁺, 309.7 [M–4PF₆]⁴⁺.

Complex [(DMBP)₂Ru(bpy-NO₂)](PF₆)₃ (3-bpy**):** This complex was synthesized and purified following a procedure adapted from the one described for **0-bpy**. To a solution of [(dmbp)₂RuCl₂] (0.23 g, 0.426 mmol) in

CH_2Cl_2 (5 mL), $\text{NO}_2\text{-bpy}$ (0.103 g, 0.511 mmol, 1.2 equiv) and EtOH (45 mL) were added, and the mixture was heated to reflux for 20 h under inert atmosphere (Ar). After the mixture had cooled, H_2O (55 mL) and an excess of NH_4PF_6 salt (0.350 g, 2.13 mmol, 5 equiv/Ru) were added, whilst vigorously stirring, to precipitate the complex. The product was filtered off, washed successively with H_2O , EtOH, and Et_2O , to give a dark red/violet solid. The product was purified by column chromatography over basic alumina by using an eluent of increasing polarity: $\text{EtOAc}/\text{CH}_2\text{Cl}_2$ 100:0 \rightarrow 0:100, then with a mixture of CH_2Cl_2 /acetone 100:0 \rightarrow 0:100. The final recrystallization was performed by slow diffusion of Et_2O in a concentrated acetonitrile solution of the complex, affording pure **3-bpy** as a dark red-violet microcrystalline solid (0.27 g, 65%). The racemic mixture ($\Lambda + \Delta$) was not resolved. ^1H NMR (250 MHz, CD_3CN): δ = 9.12 (d, $^4J(\text{H}^3, \text{H}^5)$ = 2.0 Hz, 1H; H^3), 8.73 (d, $^3J(\text{H}^3, \text{H}^4)$ = 8.1 Hz, 1H; H^3), 8.39 (s, 4H; $\text{H}^{3, \text{DMBP}}$), 8.12 (m, 2H; H^6 , H^4), 7.99 (dd, $^3J(\text{H}^5, \text{H}^6)$ = 6.2 Hz, $^4J(\text{H}^5, \text{H}^3)$ = 2.2 Hz 1H; H^5), 7.81 (d, $^3J(\text{H}^6, \text{H}^5)$ = 5.3 Hz, 1H; H^6), 7.51 (m, 5H; H^5 , $\text{H}^{5, \text{DMBP}}$), 7.26 (m, 4H; $\text{H}^{5, \text{DMBP}}$), 2.57 (s, 6H; $\text{H}^{\text{Me, DMBP}}$), 2.56 ppm (s, 6H; $\text{H}^{\text{Me, DMBP}}$); elemental analysis (%) calcd for $\text{C}_{34}\text{H}_{31}\text{N}_7\text{O}_2\text{RuP}_2\text{F}_{12}\cdot\text{H}_2\text{O}$: C 41.73, H 3.40, N 10.02; found: C 41.38, H 3.67, N 9.84; ES-MS: m/z : 816.0 $[\text{M}-\text{PF}_6]^-$, 335.7 $[\text{M}-2\text{PF}_6]^{2+}$.

Complex [(DMBP)₂Ru(bpy-(NO₂)₂)(PF₆)₂ (4-bpy): The synthetic method was the same as the one reported for **3-bpy**, by using [(dmdbp)₂RuCl₂] (0.21 g, 0.389 mmol) in CH_2Cl_2 (5 mL) and $(\text{NO}_2)_2\text{-bpy}$ (0.115 g, 0.467 mmol, 1.2 equiv), to give the pure **4-bpy** compound as dark brown crystals (0.189 g, 47.5%). The racemic mixture ($\Lambda + \Delta$) was not resolved. ^1H NMR (250 MHz, CD_3CN): δ = 9.39 (d, $^4J(\text{H}^3, \text{H}^5)$ = 2.1 Hz, 2H; H^3), 8.41 (s, 2H; $\text{H}^{3, \text{DMBP}}$) + 8.40 (s, 2H; $\text{H}^{3, \text{DMBP}}$), 8.18 (d, $^3J(\text{H}^6, \text{H}^5)$ = 6.3 Hz, 2H; H^6), 8.09 (dd, $^3J(\text{H}^5, \text{H}^6)$ = 6.3 Hz, $^4J(\text{H}^5, \text{H}^3)$ = 2.2 Hz 2H; H^5), 7.50 (d, $^3J(\text{H}^{6, \text{DMBP}}, \text{H}^{5, \text{DMBP}})$ = 5.8 Hz, 2H; $\text{H}^{6, \text{DMBP}}$) + 7.46 (d, $^3J(\text{H}^{6, \text{DMBP}}, \text{H}^{5, \text{DMBP}})$ = 5.8 Hz, 2H; $\text{H}^{6, \text{DMBP}}$), 7.33 (d, $^3J(\text{H}^{5, \text{DMBP}}, \text{H}^{6, \text{DMBP}})$ = 5.8 Hz, 2H; $\text{H}^{5, \text{DMBP}}$) + 7.26 (d, $^3J(\text{H}^{6, \text{DMBP}}, \text{H}^{5, \text{DMBP}})$ = 5.6 Hz, 2H; $\text{H}^{6, \text{DMBP}}$), 2.59 (s, 6H; $\text{H}^{\text{Me, DMBP}}$), 2.56 ppm (s, 6H; $\text{H}^{\text{Me, DMBP}}$); elemental analysis (%) calcd for $\text{C}_{34}\text{H}_{30}\text{N}_8\text{O}_4\text{RuP}_2\text{F}_{12}\cdot\text{H}_2\text{O}$: C 39.89, H 3.15, N 10.95; found: C 40.10, H 3.38, N 10.67; ES-MS: m/z : 861.0 $[\text{M}-\text{PF}_6]^-$, 358.1 $[\text{M}-2\text{PF}_6]^{2+}$.

X-ray Crystal structure determinations: Crystals of inorganic compounds (**1-bpy** and **2-bpy**) were grown by slow diffusion of diethyl ether into acetonitrile solutions of the complexes whereas single crystals of **A₂-bpy** were obtained by slow evaporation of an acetonitrile solution of the organic ligand. Intensity data were collected for **A₂-bpy**, **1-bpy** and **2-bpy** on a Bruker-Nonius Kappa CCD diffractometer (MoK_{α} , λ = 0.71069 Å, graphite monochromator) with sample-to-detector distances of 40 mm. They covered the whole sphere of reciprocal space by rotating in ϕ about 1°. Frames were integrated and corrected for Lorentz and polarization effects using DENZO. The scaling as well as refinements of cell parameters were performed by SCALEPACK. The structures were solved by direct methods and refined by full-matrix least squares based on F^2 by using the SHELXTL-PLUS program. Hydrogen atoms were included in calculated positions according to a riding model. No hydrogen atom was introduced for solvent molecules in the structures of the two complexes. CCDC-184581 (**1-bpy**), -254423 (**2-bpy**) and -254422 (**A₂-bpy**) contain the supplementary crystallographic data for this paper. These data can be obtained free of charge from The Cambridge Crystallographic Data Centre via www.ccdc.cam.ac.uk/data_request/cif

Crystal data for **1-bpy**: ($\text{C}_{57}\text{H}_{48}\text{N}_7\text{Ru}$)($3(\text{PF}_6)$ ·0.5($\text{C}_4\text{H}_{10}\text{O}$), M = 1404.07, triclinic, $P\bar{1}$, a = 11.8592(1), b = 15.5583(3), c = 19.5193(4) Å, α = 101.344(1), β = 95.037(1), γ = 111.568(1)°, V = 3232.7(2) Å³, Z = 2, ρ_{calcd} = 1.435 g cm⁻³, μ = 0.41 mm⁻¹; T = 293 K, 27858 observed reflections ($2\theta_{\text{max}}$ = 52°, $R(\text{int})$ = 0.07). Crystal dimensions: 0.38 × 0.28 × 0.25 mm. A two-fold orientational disorder was evidenced for the 3 PF_6 anions, their major populations coefficients were refined to 0.842, 0.756 and 0.866, respectively. Appropriate restraints were defined (σ = 0.03). Due to a pronounced disorder, the populations of the diethyl oxide carbon atoms were fixed to 0.5 or 0.25. Similarity, planarity, and bond lengths restraints were applied to the complex (σ = 0.03). Anisotropic least-square refinements were carried out for all non-hydrogen atoms, except for the minor populations of the PF_6 anions and for the carbon atoms of the Et_2O molecule, which were refined isotropically. Refinements: $R[F^2 > 2\sigma(F^2)]$ =

0.0692, R (all data) = 0.1892, $wR2$ (all data) = 0.1403, S = 1.038 for 12634 independent reflections, 2283 restraints and 852 parameters, largest peak/hole 0.42/−0.29 e Å⁻³.

Crystal data for **2-bpy**: ($\text{C}_{80}\text{H}_{64}\text{N}_8\text{Ru}$)($4(\text{PF}_6)$ ·5(CH_3CN)·1.5(H_2O), M = 2032.49, triclinic, $P\bar{1}$, a = 14.8025(2), b = 16.5875(2), c = 20.5806(2) Å, α = 69.724(1), β = 78.565(1), γ = 83.956(1)°, V = 4642.5(16) Å³, Z = 2, ρ_{calcd} = 1.454 g cm⁻³, μ = 0.335 mm⁻¹, T = 140.0(5) K, 119099 observed reflections ($2\theta_{\text{max}}$ = 63°, $R(\text{int})$ = 0.054). Crystal dimensions: 0.22 × 0.12 × 0.08 mm. Bond lengths (σ = 0.02), and similarity (σ = 0.04) restraints were applied to the whole complex. The pyridine and phenyl rings were restrained to C_{6h} symmetry (σ = 0.2). Isotropic (σ = 0.03), and bond lengths (σ = 0.03) restraints were applied to the counter-anions and to the solvent molecules. The fluorine atoms of two PF_6 counter-anions are disordered, in one case four, and in the other all six fluorine atoms are distributed over two positions. All cocrystallized solvent molecules except one acetonitrile molecule are disordered or have partial occupancy. It was also necessary to define three water positions close to an acetonitrile to fit the electronic density. Three acetonitrile and all water molecules were refined with isotropic atomic displacement parameters. Refinements: $R[F^2 > 2\sigma(F^2)]$ = 0.088, R (all data) = 0.118, $wR2$ (all data) = 0.253, S = 1.65 for 29332 data, 3675 restraints and 1326 parameters. Final difference Fourier synthesis shows two maxima (2.0 and 1.2 e Å⁻³) close (0.66 and 0.78 Å) to the position of the Ru atom, similarly to the crystal structure of a previously reported tetracationic bis-terpyridyl ruthenium complex **P1A₂/Ru**.^[10b] This feature may indicate that the crystal contain a minor twin component. The next maxima of residual electronic densities stand in the expected range (< 1 e Å⁻³).

Crystal data for **A₂-bpy**: ($\text{C}_{56}\text{H}_{40}\text{N}_4$)($2(\text{BF}_4)$ ·2(CH_3CN)·1/8(H_2O), M = 1026.65, triclinic, $P\bar{1}$, a = 14.9050(3), b = 18.0678(3), c = 20.8380(5) Å, α = 110.465(1), β = 89.874(2), γ = 101.083(2)°, V = 5146.54(18) Å³, Z = 4, ρ_{calcd} = 1.325 g cm⁻³, μ = 0.098 mm⁻¹, T = 150.0(5) K, 55596 observed reflections ($2\theta_{\text{max}}$ = 50°, $R(\text{int})$ = 0.075). Crystal dimensions: 0.25 × 0.22 × 0.20 mm. The asymmetric unit is made up of two bis-acceptor ligands that show weak geometrical dissimilarities. Among the four BF_4 counter-anions, all but one are disordered, whereas the four independent acetonitrile molecules are well ordered. An isolated maximum of electronic density was attributed to a water molecule with partial occupancy, its population refine to 1/4. Similarity, planarity, and bond lengths restraints were applied to the ligands (σ = 0.03), and to the counter-anions (σ = 0.02), acetonitrile bond lengths were restrained to standard target values (σ = 0.03). The positions of the nitrogen atoms on the bipyridine were unambiguously determined. Refinements: $R[F^2 > 2\sigma(F^2)]$ = 0.092, R (all data) = 0.157, $wR2$ (all data) = 0.241, S = 1.13 for 18113 data, 2564 restraints and 1465 parameters, largest peak/hole 0.70/−0.51 e Å⁻³.

Electrochemical measurements: The electrochemical experiments were carried out with a conventional three-electrodes cell (solution volume of 15 mL) and a PC-controlled potentiostat/galvanostat (Princeton Applied Research Inc. model 263 A). The working electrode was a vitreous carbon electrode from Radiometer-Tacussel exposing a geometrical area of 0.071 cm² and mounted in Teflon. The electrode was polished before each experiment with 3 and 0.3 μm alumina pastes followed by extensive rinsing with ultrapure Milli-Q water. Platinum wire was used as counter electrode and saturated calomel electrode, SCE, as reference electrode. Electrolytic solutions, acetonitrile containing tetrabutylammonium tetrafluoroborate 0.1 M (TBABF₄, Aldrich, +99%) as supporting electrolyte, were routinely deoxygenated by argon bubbling. All the potential values are given versus the calomel saturated electrode SCE. Cyclic voltammetric data were used to estimate formal potentials $E_{1/2}$ as $(E_{\text{pa}} + E_{\text{pc}})/2$, where E_{pa} and E_{pc} are the anodic and cathodic peak potentials related to the considered redox process.

Photophysical properties: The uncorrected emission spectra were obtained with a Jobin Yvon Spex Fluorolog FL 111 spectrofluorimeter. Emission quantum yields for argon-degassed acetonitrile solutions of the complexes were determined relative to an acetonitrile solution of $[\text{Ru}(\text{bpy})_3]^{2+}$ by using $\Phi_{\text{em}} = 6.2 \times 10^{-2}$ as a reference.^[74] Excitation spectra were corrected from the lamp spectrum. The optical density of each solution was adjusted to 0.1 at the excitation wavelength.

Excited state lifetimes were determined by laser flash spectroscopy. Briefly, the nanosecond setup is based on an excimer laser (Lambda Physik EMG 100, 308 nm pulses of duration 10 ns and energy 150 mJ), which was used as excitation source. The detection system consisted of a Jobin Yvon H25 monochromator, a Hamamatsu R955 photomultiplier and a Le Croy 9362 digital oscilloscope. The laser intensity was attenuated to avoid biphotonic effects. The analysis was carried out within the first millimeter of the sample excited by the laser pulse, using quartz cells of 1 cm path length (room temperature exp.). The optical density of samples was adjusted to 0.8 at the excitation wavelength of the laser ($\lambda_{\text{exc}} = 308$ nm). All photophysical properties have been determined in acetonitrile (Aldrich, 99.5 %, spectrophotometric grade) at room temperature and in butyronitrile (Aldrich, 99+ %) at 77 K. At low temperature, we used cylindrical quartz cells and the solutions were cooled in a quartz Dewar containing liquid nitrogen. Solutions were deaerated either by bubbling with argon (room temperature exp.) or by vacuum degassing with successive freeze-pump-thaw cycles (low temperature exp.).

Computational method: All calculations were carried out by using the Gaussian code.^[75] A hybrid Hartree–Fock/density functional model, hereafter PBE0, was used throughout.^[76] In this functional, derived from the PBE,^[77] the ratio of HF/DFT exchange is fixed a priori to $1/4$.^[78] A double ξ quality LANL2 basis^[79] and corresponding pseudo-potential^[80] was used for all calculations. Such a level of theory was proven to provide reliable results both for thermochemical and spectroscopic properties.^[28] No symmetry constraints were applied and, in the case of reduced systems, unrestricted calculations were performed and spin contamination, monitored by the S^2 expectation value, was found to be negligible. Unless otherwise specified the X-ray crystallographic structures were used and counteranions were not taken into account.

When referring to spin density, Mulliken spin distributions are considered.

Acknowledgements

We thank V. Albin for performing electrochemical measurements and Dr. G. Bertho for his support regarding the NMR study; we are also indebted to Prof. F. Scandola and Dr. C. Chiorboli for femtosecond^[57] transient absorption experiments.

- [1] a) V. Balzani, L. Moggi, F. Scandola, *Supramolecular Photochemistry* (Ed.: V. Balzani), D. Reidel Publishing Company, **1987**, pp. 1–28; b) T. J. Meyer, *Acc. Chem. Res.* **1989**, *22*, 163–170; c) J.-M. Lehn, *Angew. Chem.* **1990**, *102*, 1347; *Angew. Chem. Int. Ed. Engl.* **1990**, *29*, 1304–1319.
- [2] H. Imahori, M. Kimura, K. Hosomizu, T. Sato, T. K. Ahn, S. K. Kim, D. Kim, Y. Nishimura, I. Yamazaki, Y. Araki, O. Ito, S. Fukuzumi, *Chem. Eur. J.* **2004**, *10*, 5111–5122.
- [3] N. Hirata, J.-J. Lagref, E. J. Palomares, J. R. Durrant, M. K. Nazeeruddin, M. Gratzel, D. Di Cenzo, *Chem. Eur. J.* **2004**, *10*, 595–602.
- [4] D. Gust, T. A. Moore, A. L. Moore, *Acc. Chem. Res.* **2001**, *34*, 40–48.
- [5] H. Kurreck, M. Huber, *Angew. Chem.* **1995**, *107*, 929–947; *Angew. Chem. Int. Ed. Engl.* **1995**, *34*, 849–866.
- [6] a) S. E. Miller, A. S. Lukas, E. Marsh, P. Bushard, M. R. Wasielewski, *J. Am. Chem. Soc.* **2000**, *122*, 7802–7810; b) F. Vögtle, M. Frank, M. Neger, P. Belser, A. von Zelewsky, V. Balzani, F. Barigelli, L. De Cola, L. Flamigni, *Angew. Chem.* **1993**, *105*, 1706–1709; *Angew. Chem. Int. Ed. Engl.* **1993**, *32*, 1643–1646.
- [7] a) V. Balzani, A. Juris, M. Venturi, S. Campagna, S. Serroni, *Chem. Rev.* **1996**, *96*, 759–833; b) V. Balzani, F. Scandola, *Supramolecular Photochemistry*, Ellis Horwood, Chichester, **1991**.
- [8] a) E. Baranoff, J.-P. Collin, L. Flamigni, J.-P. Sauvage, *Chem. Soc. Rev.* **2004**, *33*, 147–155; b) I. M. Dixon, J.-P. Collin, J.-P. Sauvage, F. Barigelli, L. Flamigni, *Angew. Chem.* **2000**, *112*, 1348–1351; *Angew. Chem. Int. Ed.* **2000**, *39*, 1292–1295; c) J.-P. Collin, P. Gaviña, V. Heitz, J.-P. Sauvage, *Eur. J. Inorg. Chem.* **1998**, 1–14; d) F. Barigelli, L. Flamigni, J.-P. Collin, J.-P. Sauvage, *Chem. Commun.* **1997**, 333–338; e) J.-P. Sauvage, J.-P. Collin, J.-C. Chambron, S. Guillerez, C. Coudret, V. Balzani, F. Barigelli, L. De Cola, L. Flamigni, *Chem. Rev.* **1994**, *94*, 993–1019.
- [9] Our work is mainly focussed on inorganic assemblies and restricted to non-porphyrinic systems.
- [10] a) P. Lainé, F. Bedioui, E. Amouyal, V. Albin, F. Berruyer-Penaud, *Chem. Eur. J.* **2002**, *8*, 3162–3176; b) P. Lainé, F. Bedioui, P. Ochsenbein, V. Marvaud, M. Bonin, E. Amouyal, *J. Am. Chem. Soc.* **2002**, *124*, 1364–1377.
- [11] a) H. Dürr, S. Bossmann, *Acc. Chem. Res.* **2001**, *34*, 905–917; b) T. J. Meyer, *Pure Appl. Chem.* **1990**, *62*, 1003–1009.
- [12] There exists, however, a few examples of bridging units exhibiting at one and the same time rigid features and insulating properties, like adamantyl-based spacers, but they are also synthetically demanding: a) G. Albano, P. Belser, C. Daul, *Inorg. Chem.* **2001**, *40*, 1408–1413; b) L. De Cola, P. Belser, *Coord. Chem. Rev.* **1998**, *177*, 301–346.
- [13] D. Holten, D. F. Bocian, J. S. Lindsey, *Acc. Chem. Res.* **2002**, *35*, 57–69.
- [14] O. Johansson, M. Borgström, R. Lomoth, M. Palmblad, J. Bergquist, L. Hammarström, L. Sun, B. Åkermarck, *Inorg. Chem.* **2003**, *42*, 2908–2918.
- [15] A. Juris, V. Balzani, F. Barigelli, S. Campagna, P. Belser, A. von Zelewsky, *Coord. Chem. Rev.* **1988**, *84*, 85–277.
- [16] C. Chiorboli, S. Fracasso, F. Scandola, S. Campagna, S. Serroni, R. Konduri, F. McDonnell, *Chem. Commun.* **2003**, 1658–1659.
- [17] a) M. D. Ward, *Chem. Soc. Rev.* **1995**, *24*, 121–134; b) D. T. Pierce, W. E. Geiger, *Inorg. Chem.* **1994**, *33*, 373–381; c) T.-Y. Dong, C.-H. Huang, C.-K. Chang, Y.-S. Wen, S.-L. Lee, J.-A. Chen, W.-Y. Yeh, A. Yeh, *J. Am. Chem. Soc.* **1993**, *115*, 6357–6368; d) P. Chen, M. Curry, T. J. Meyer, *Inorg. Chem.* **1989**, *28*, 2271–2280; e) S. Larson, *J. Am. Chem. Soc.* **1981**, *103*, 4034–4040; f) H. Fisher, G. M. Tom, H. Taube, *J. Am. Chem. Soc.* **1976**, *98*, 5512–5517.
- [18] a) A. Gourdon, *New J. Chem.* **1992**, *16*, 953–957; b) S. Woitellier, J.-P. Launay, C. Joachim, *Chem. Phys.* **1989**, *131*, 481–488; c) C. Joachim, J.-P. Launay, *Chem. Phys.* **1986**, *109*, 93–99.
- [19] a) A. C. Benniston, A. Harriman, P. Li, C. A. Sams, M. D. Ward, *J. Am. Chem. Soc.* **2004**, *126*, 13630–13631; b) A. C. Benniston, A. Harriman, P. Li, C. A. Sams, *Tetrahedron Lett.* **2003**, *44*, 4167–4169.
- [20] C. Berg-Brennan, P. Subramanian, M. Absi, C. Stern, J. T. Hupp, *Inorg. Chem.* **1996**, *35*, 3719–3722.
- [21] a) N. W. Alcock, P. R. Barker, J. M. Haider, M. J. Hannon, C. L. Painting, Z. Pikramenou, E. A. Plummer, K. Rissanen, P. Saarenketo, *J. Chem. Soc. Dalton Trans.* **2000**, 1447–1461; b) M. L. Scudder, H. A. Goodwin, I. G. Dance, *New J. Chem.* **1999**, *23*, 695–705.
- [22] Peculiar angle θ^1 of 64.05° within **2-bpy** is excluded; see NMR study.
- [23] I. S. A. Farag, A. I. El-Shora, V. B. Rybakov, *Cryst. Res. Technol.* **1990**, *25*, 519–524.
- [24] A. H. Othman, Z. Zakaria, S. W. Ng, *J. Crystallogr. Spectrosc. Res.* **1993**, *23*, 921.
- [25] H.-T. Zhang, S. G. Yan, P. Subramanian, L. M. Skeens-Jones, C. Stern, J. T. Hupp, *J. Electroanal. Chem.* **1996**, *414*, 23–29.
- [26] J. S. Lamba, C. L. Fraser, *J. Am. Chem. Soc.* **1997**, *119*, 1801–1802.
- [27] The detailed analysis of the temperature dependence of ^1H NMR spectra of compounds **1-bpy** and **2-bpy** will be reported elsewhere, the work is in progress.
- [28] I. Ciofini, P. P. Lainé, F. Bedioui, C. Adamo, *J. Am. Chem. Soc.* **2004**, *126*, 10763–10777.
- [29] M. B. Smith, J. March, *March's Advanced Organic Chemistry: Reactions, Mechanisms, and Structure*, 5th ed., Wiley, **2001**.
- [30] M. J. Cook, A. P. Lewis, G. S. G. McAuliffe, V. Skarda, A. J. Thomson, J. L. Glasper, D. J. Robbins, *J. Chem. Soc. Perkin Trans. 2* **1984**, 1293–1301.
- [31] M. Pilkington, S. Capelli, J. Hauser, C. Hoffmann, H.-B. Bürgi, *Acta Crystallogr. Sect. C* **1997**, *53*, 1719–1721.

- [32] A. Juris, F. Barigelletti, V. Balzani, P. Belser, A. von Zelewsky, *Isr. J. Chem.* **1982**, 22, 87–90.
- [33] This possibility of tuning the properties of MLCT excited states is of interest for building panchromatic (black) absorbers to better overlap with solar emission spectrum; see a) M. Grätzel, *J. Photochem. Photobiol. C* **2003**, 4, 145–153; b) P. A. Anderson, F. R. Keen, T. J. Meyer, J. A. Moss, G. F. Strouse, *J. Chem. Soc. Dalton Trans.* **2002**, 3820–3831.
- [34] a) J. V. Caspar, T. J. Meyer, *Inorg. Chem.* **1983**, 22, 2444–2453; b) J. V. Caspar, T. J. Meyer, *J. Am. Chem. Soc.* **1983**, 105, 5583–5590; c) E. M. Kober, J. L. Marshall, W. J. Dressick, B. P. Sullivan, J. V. Caspar, T. J. Meyer, *Inorg. Chem.* **1985**, 24, 2755–2763.
- [35] $E(\text{MLCT1}) = 0.578(\Delta E_{1/2}) + 1.251$, $R = 0.985$; $E(\text{MLCT2}) = -0.846(\Delta E_{1/2}) + 4.878$, $R = 0.998$; $E_{\text{em}}(77 \text{ K}) = -0.703(\Delta E_{1/2}) + 3.902$, $R = 0.997$; $E_{\text{em}}(298 \text{ K}) = -0.701(\Delta E_{1/2}) + 3.774$, $R = 0.998$.
- [36] J. K. Nagle, J. S. Bernstein, R. C. Young, T. J. Meyer, *Inorg. Chem.* **1981**, 20, 1760–1764.
- [37] At RT, $\Delta E_{\text{em}}(0-1) = 1185 \text{ cm}^{-1}$ and $\Delta E_{\text{em}}(1-2) = 1022 \text{ cm}^{-1}$; at 77 K, $\Delta E_{\text{em}}(0-1) = 1234 \text{ cm}^{-1}$ and $\Delta E_{\text{em}}(1-2) = 980 \text{ cm}^{-1}$.
- [38] Y. Shen, K. A. Walters, K. Abboud, K. S. Schanze, *Inorg. Chim. Acta* **2000**, 300–302, 414–426.
- [39] M. Maestri, N. Armaroli, V. Balzani, E. C. Constable, A. M. W. Cargill Thompson, *Inorg. Chem.* **1995**, 34, 2759–2767.
- [40] Y.-Q. Fang, N. J. Taylor, G. S. Hanan, F. Loiseau, R. Passalacqua, S. Campagna, H. Nierengarten, A. Van Dorsselaer, *J. Am. Chem. Soc.* **2002**, 124, 7912–7913.
- [41] F. Scandola, C. Chiorboli: personal communication.
- [42] P. Belser, A. von Zelewsky, A. Juris, F. Barigelletti, V. Balzani, *Chem. Phys. Lett.* **1984**, 104, 100–104.
- [43] a) D. J. Liard, M. Busby, I. R. Farrell, P. Matousek, M. Towrie, A. Vlcek Jr., *J. Phys. Chem. A* **2004**, 108, 556–567; b) N. H. Damrauer, J. K. McCusker, *J. Phys. Chem. A* **1999**, 103, 8440–8446; c) N. H. Damrauer, T. R. Boussie, M. Devenney, J. McCusker, *J. Am. Chem. Soc.* **1997**, 119, 8253–8268.
- [44] P. D. Beer, Z. Chen, A. Grieve, J. Haggitt, *J. Chem. Soc. Chem. Commun.* **1994**, 2413–2414.
- [45] G. F. Strouse, J. R. Schoonover, R. Duesing, S. Boyde, W. E. Jones, Jr., T. J. Meyer, *Inorg. Chem.* **1995**, 34, 473–487.
- [46] a) J.-F. Guillemoles, V. Barone, L. Joubert, C. Adamo, *J. Phys. Chem. A* **2002**, 106, 11354–11360; b) C. Adamo, V. Barone, G. E. Scuseria, *J. Chem. Phys.* **1999**, 111, 2889–2899.
- [47] J. McCusker, *Acc. Chem. Res.* **2003**, 36, 876–887.
- [48] J. C. Luong, L. Nadjio, M. S. Wrighton, *J. Am. Chem. Soc.* **1978**, 100, 5790–5795; this statement is in reference to previously discussed actual electronic expanse of the acceptor moiety; see also refs. [10] and [28].
- [49] R. Passalacqua, F. Loiseau, S. Campagna, Y.-Q. Fang, G. S. Hanan, *Angew. Chem.* **2003**, 115, 1645–1649; *Angew. Chem. Int. Ed.* **2003**, 42, 1607–1611.
- [50] M. B. Robin, P. Day, *Adv. Inorg. Chem. Radiochem.* **1967**, 10, 247–422.
- [51] a) B. S. Brunschwig, C. Creutz, N. Sutin, *Chem. Soc. Rev.* **2002**, 31, 168–184; b) K. D. Demadis, C. M. Hartshorn, T. J. Meyer, *Chem. Rev.* **2001**, 101, 2655–2685.
- [52] A. C. Benniston, A. Harriman, P. Li, C. A. Sams, *Phys. Chem. Chem. Phys.* **2004**, 6, 875–877.
- [53] F. Barigelletti, L. Flamigni, *Chem. Soc. Rev.* **2000**, 29, 1–12.
- [54] J.-P. Launay, *Chem. Soc. Rev.* **2001**, 30, 386–397.
- [55] a) E. Amouyal, A. Homs, J.-C. Chambron, J.-P. Sauvage, *J. Chem. Soc. Dalton Trans.* **1990**, 1841–1845; b) M. K. Brennaman, J. H. Alstrum-Acevedo, C. N. Fleming, P. Jang, T. J. Meyer, J. M. Papanikolas, *J. Am. Chem. Soc.* **2002**, 124, 15094–15098; c) G. Pourtois, D. Beljonne, C. Moucheron, S. Schumm, A. Kirsch-De-Mesmaeker, R. Lazzaroni, J.-L. Brédas, *J. Am. Chem. Soc.* **2004**, 126, 683–692.
- [56] a) E. Ishow, A. Gourdon, J.-P. Launay, C. Chiorboli, F. Scandola, *Inorg. Chem.* **1999**, 38, 1504–1510; b) J. Bolger, A. Gourdon, E. Ishow, J.-P. Launay, *Inorg. Chem.* **1996**, 35, 2937–2944.
- [57] C. Chiorboli, M. A. J. Rodgers, F. Scandola, *J. Am. Chem. Soc.* **2003**, 125, 483–491.
- [58] a) R. Konduri, N. R. de Tacconi, K. Rajeshwar, F. M. MacDonnell, *J. Am. Chem. Soc.* **2004**, 126, 11621–11629; b) R. Konduri, H. Ye, F. M. MacDonnell, S. Serroni, S. Campagna, K. Rajeshwar, *Angew. Chem.* **2002**, 114, 3317–3319; *Angew. Chem. Int. Ed.* **2002**, 41, 3185–3187; c) M.-J. Kim, R. Konduri, H. Ye, F. M. MacDonnell, F. Puntoriero, S. Serroni, S. Campagna, T. Holder, G. Kinsel, K. Rajeshwar, *Inorg. Chem.* **2002**, 41, 2471–2476; d) L. Flamigni, S. Encinas, F. Barigelletti, F. M. MacDonnell, K.-J. Kim, F. Puntoriero, S. Campagna, *Chem. Commun.* **2000**, 1185–1186.
- [59] Y. Pellegrin, K. E. Berg, G. Blondin, E. Anxolabéhère-Mallart, W. Lielbl, A. Aukauloo, *Eur. J. Inorg. Chem.* **2003**, 1900–1910.
- [60] a) K. Ohkubo, H. Kotani, J. Shao, Z. Ou, K. M. Kadish, G. Li, R. K. Pandey, M. Fujitsuka, O. Ito, H. Imahori, S. Fukuzumi, *Angew. Chem.* **2004**, 116, 871–874; *Angew. Chem. Int. Ed.* **2004**, 43, 853–856; b) S. Fukuzumi, H. Kotani, K. Ohkubo, S. Ogo, N. V. Tkachenko, H. Lemmetyinen, *J. Am. Chem. Soc.* **2004**, 126, 1600–1601.
- [61] A. Harriman, *Angew. Chem.* **2004**, 116, 5093–5095; *Angew. Chem. Int. Ed.* **2004**, 43, 4985–4987.
- [62] W. B. Davis, M. A. Ratner, M. R. Wasielewski, *J. Am. Chem. Soc.* **2001**, 123, 7877–7886.
- [63] T. Ueno, Y. Urano, K. Setsukinai, H. Takakusa, H. Kojima, K. Kikuchi, K. Ohkubo, S. Fukuzumi, T. Nagano, *J. Am. Chem. Soc.* **2004**, 126, 14079–14085.
- [64] J. A. Simon, S. L. Curry, R. H. Schmehl, T. R. Schatz, P. Piotrowiak, X. Jin, R. P. Thummel, *J. Am. Chem. Soc.* **1997**, 119, 11012–11022.
- [65] D. S. Tyson, C. A. Bignozzi, F. N. Castellano, *J. Am. Chem. Soc.* **2002**, 124, 4562–4563.
- [66] S. K. Pati, T. J. Marks, M. A. Ratner, *J. Am. Chem. Soc.* **2001**, 123, 7287–7291.
- [67] B. J. Coe, *Chem. Eur. J.* **1999**, 5, 2464–2471, and references therein.
- [68] M. Konstantaki, E. Koudoumas, S. Couris, P. Lainé, E. Amouyal, S. Leach, *J. Phys. Chem. B* **2001**, 105, 10797–10804.
- [69] R. Alan Jones, B. D. Roney, W. H. F. Sasse, K. O. Wade, *J. Chem. Soc. B* **1967**, 106–111.
- [70] a) D. Wenkert, R. B. Woodward, *J. Org. Chem.* **1983**, 48, 283–289; b) X. Sun, Y.-K. Yang, F. Lu, *Macromol. Chem. Phys.* **1997**, 198, 833–841; c) J. Haginiwa, *J. Pharm. Soc. Japan* **1955**, 75, 731–733; d) J. Haginiwa, *J. Pharm. Soc. Japan* **1955**, 75, 733–736; e) I. Murase, *Nippon Kagaku Zasshi* **1956**, 77, 682–685.
- [71] T. Q. Nguyen, F. Qu, X. Huang, A. F. Janzen, *Can. J. Chem.* **1992**, 70, 2089–2093.
- [72] a) G. Maerker, F. H. Case, *J. Am. Chem. Soc.* **1958**, 80, 2745–2748; b) D. St. C. Black, N. E. Rothnie, *Aust. J. Chem.* **1983**, 36, 1141–1147; c) R.-A. Fallahpour, M. Neuburger, M. Zehnder, *New J. Chem.* **1999**, 23, 53–61; d) R. A. Fallahpour, *Eur. J. Inorg. Chem.* **1998**, 1205–1207.
- [73] a) P. A. Lay, A. M. Sargeson, H. Taube, *Inorg. Synth.* **1986**, 24, 291–299; b) B. P. Sullivan, D. J. Salmon, T. J. Meyer, *Inorg. Chem.* **1978**, 17, 3334–3341.
- [74] J. M. Calvert, J. V. Caspar, R. A. Binstead, T. D. Westmoreland, T. J. Meyer, *J. Am. Chem. Soc.* **1982**, 104, 6620–6627.
- [75] Gaussian Development Version, Revision A.01, M. J. Frisch, G. W. Trucks, H. B. Schlegel, G. E. Scuseria, M. A. Robb, J. R. Cheeseman, J. A. Montgomery, Jr., T. Vreven, K. N. Kudin, J. C. Burant, J. M. Millam, S. S. Iyengar, J. Tomasi, V. Barone, B. Mennucci, M. Cossi, G. Scalmani, N. Rega, G. A. Petersson, H. Nakatsuji, M. Hada, M. Ehara, K. Toyota, R. Fukuda, J. Hasegawa, M. Ishida, T. Nakajima, Y. Honda, O. Kitao, H. Nakai, X. Li, J. E. Knox, H. P. Hratchian, J. B. Cross, C. Adamo, J. Jaramillo, R. Gomperts, R. E. Stratmann, R. Cammi, C. Pomelli, J. Ochterski, P. Y. Ayala, K. Morokuma, W. L. Hase, P. Salvador, J. J. Dannenberg, V. G. Zakrzewski, S. Dapprich, A. D. Daniels, M. C. Strain, O. Farkas, D. K. Malick, A. D. Rabuck, K. Raghavachari, J. B. Foresman, J. V. Ortiz, Q. Cui, A. G. Baboul, S. Clifford, J. Cioslowski, B. B. Stefanov, G. Liu, A. Liashenko, P. Piskorz, I. Komaromi, R. L. Martin, D. J. Fox, T. Keith, M. A. Al-Laham, C. Y. Peng, A. Nanayakkara, M. Challacombe, P. M. W.

- Gill, B. Johnson, W. Chen, M. W. Wong, C. Gonzalez, J. A. Pople, Gaussian, Inc., Pittsburgh PA, **2003**.
- [76] C. Adamo, V. Barone, *J. Chem. Phys.* **1999**, *110*, 6158–6170.
- [77] J. P. Perdew, K. Burke, M. Ernzerhof, *Phys. Rev. Lett.* **1996**, *77*, 3865–3868.
- [78] C. Adamo, V. Barone, *Chem. Phys. Lett.* **1997**, *274*, 242–250.
- [79] T. H. Dunning Jr., P. J. Hay, in *Modern Theoretical Chemistry* (Ed.: H. F. Schaefer III), Plenum, New York, 1976, pp. 1–28.
- [80] P. J. Hay, W. R. Wadt, *J. Chem. Phys.* **1985**, *82*, 299–310.

Received: November 15, 2004

Published online: April 8, 2005